

AN ELASTIC REBOUND MODEL FOR
NORMAL FAULT EARTHQUAKES

RICHARD ANTHONY KOSELUK

A THESIS SUBMITTED IN PARTIAL FULFILLMENT
OF THE REQUIREMENTS FOR
THE MASTER OF ARTS DEGREE IN GEOLOGY,
COLLEGE OF LIBERAL ARTS,
TEMPLE UNIVERSITY, PHILADELPHIA, PENNSYLVANIA

1978

APPROVED BY



THESIS ADVISOR

ABSTRACT

Normal fault earthquakes and interseismic (secular) displacements are generated by a visco-elastic two-dimensional finite element model. Model generated phases of crustal deformation are consistent with observed crustal deformation from repeated precise geodetic levels for the areas of Fairview Peak, Nevada and Hebgen Lake, Montana. The model fit to geodetic measurements is, in most cases, within the limits of random survey error. In this thesis I propose an elastic rebound theory for normal fault earthquakes. Model studies indicate that during the interseismic phase the ground is subject to relative doming in the vicinity of the fault which may have been interpreted by some investigators to result from magma intrusion. The rate at which doming occurs gives an indication of the asthenosphere effective viscosity, which was found to be on the order of 2.0×10^{21} poise for Fairview Peak and about 2.3×10^{21} poise for Hebgen Lake. Furthermore, interseismic model simulated extension rates are 1.36mm/yr, consistent with extension rates of greater than 0.4mm/yr observed within the Great Basin. The coseismic phase results in the uplift of the footwall block and depression of the hanging wall block as has been reported by other investigators (Savage & Hastie, 1966). The sum of the interseismic and coseismic movements result in a tilt block type of topography, as is observed in the

Basin and Range. Based on shear stress recovery the recurrence interval for these faults is on the order of 10^3 years. Thus, the Fairview Peak and Hebgen Lake faults do not present any current earthquake hazard. However, since these faults do occur in regions where sets of normal faults are common, other faults may be approaching earthquake stress levels and consequently may present current earthquake hazards in these areas.

ACKNOWLEDGEMENTS

I wish to acknowledge with gratitude the aid and guidance given by my thesis committee: Dr. Gene C. Ulmer and Dr. David E. Grandstaff. I would especially like to thank my mentor, Dr. Richard E. Bischke, for suggestions and helpful criticism during the course of study. I am also grateful to Temple University for financing my studies over the past 2 1/2 years. Computer time was supplied by The Temple University Computer Center.

In addition, I would like to thank Ms. Ev Druding, Mrs. Mildred Shapiro, and Mrs. Randy Blau for their help and kindness. I also wish to thank Ms. Alison L. Gay for typing and many helpful suggestion made during the preparation of this thesis.

DEDICATION

I would like to dedicate this work to my parents,
without whose love and understanding I could not have
continued

TABLE OF CONTENTS

<u>section</u>	<u>page</u>
Introduction.....	1
Elastic Rebound Theory and Crustal Movements.....	3
Finite Element Method.....	7
Model Formulation.....	12
Model Results.....	15
Geology, Seismicity, and Tectonics of the Fairview Peak, Nevada and Hebgen Lake, Montana Regions.....	17
Survey Data.....	22
Fairview Peak, Nevada Geodetic Data.....	23
Fairview Peak Model.....	36
Hebgen Lake, Montana Geodetic Data.....	46
Hebgen Lake Model.....	54
Discussion.....	61
Summary.....	65
Bibliography.....	67

LIST OF FIGURES

<u>figure</u>	<u>page</u>
1...Elastic Rebound Models.....	6
2...Finite Element Models.....	11
3...Map of the Tectonic Setting of the Western United States.....	21
4...1954 Nevada Earthquake Map.....	25
5...A..Fairview Peak Highway Survey Coseismic Data.... B..Model Simulated Coseismic Phase.....	28
6...USCGS Elevation Changes Along US 50 Between 1934-1955 and 1955-1967.....	30
7...USCGS Elevation Changes Along US 50 Between 1955-1967, 1967-1973, and 1955-1973.....	35
8...Coseismic Shear Stress Change Contour Map.....	40
9...Shear Stress Recovery Contour Map.....	42
10..Model Simulated Interseismic and Postseismic Phases for Fairview Peak, Nevada.....	45
11..Hebgen Lake, Montana Coseismic Data.....	49
12..Map of the Hebgen Lake Region.....	51
13..Hebgen Lake, Montana Interseismic Data.....	53
14..Hebgen Lake Model Simulated Coseismic Phase.....	56
15..Hebgen Lake Model Simulated Interseismic Phase....	60

LIST OF TABLES

table page

1...Best Fit Finite Element Model Values.....14

INTRODUCTION

H. F. Reid (1910) was one of the first people to recognize the elastic nature of the earth's crust. From fragmentary ground displacement data, Reid proposed the Elastic Rebound Theory to account for right lateral strike slip displacements at the time of the 1906 San Fransisco earthquake. Fitch and Scholz (1971) have proposed a modification of Reid's theory to account for thrust faulting at the time of the magnitude 8.2 Nankaido earthquake of December 1946. No models of normal fault earthquake cycles exist. The purpose of this thesis is to present an Elastic Rebound model consistent with tensile intraplate earthquakes.

Models of crustal deformation for strike slip, thrust, and normal faulting include two distinct phases of crustal deformation: slow storage of elastic strains and sudden release of energy in earthquakes. The strain accumulation may be caused by crustal inhomogeneities (Artyushkov, 1973), mantle convection (McKenzie & Richter, 1976), phase changes (Green & Ringwood, 1972), gravitational sliding from mid-ocean ridges (Artemjev & Artyushkov, 1971; Jacoby, 1970), or by some other mechanism. The models used for normal faulting do not distinguish between models of strain accumulation. What is important is that the lithosphere can transmit extensional or tensile stress (Elsasser, 1969).

Normal faulting results from tensional stress. My work involves a rebound mechanism consistent with normal faulting as inferred from precise geodetic vertical leveling surveys in the vicinity of the magnitude 7.1 Fairview Peak, Nevada earthquake of 1954, and in the vicinity of the magnitude 7.1 Hebgen Lake, Montana earthquake of 1959. Although these data are not complete for an entire earthquake cycle they corroborate well to model generated displacements. The agreement between model results and crustal measurements in most cases is within the limits of random survey error.

ELASTIC REBOUND THEORY AND CRUSTAL MOVEMENTS

Figure 1A is a representation of Reid's classic Elastic Rebound Theory (Reid, 1910) derived empirically from horizontal ground displacements of right lateral strike slip faulting associated with the 1906 San Francisco earthquake. The United States Coast and Geodetic Survey (USCGS) made triangulation surveys in an area that crossed the San Andreas fault beginning in 1851-1865. The area was resurveyed in the interval between 1874-1892 and again after the 1906 earthquake between 1906-1907. Results of the surveys indicated definite displacements of land took place on opposite sides of the fault, reaching a maximum at the fault surface (Fig 1A, after Reid, 1910). Reid concluded that more than half of the strain, which caused the slippage along the fault in 1906, had accumulated in a 50 year period prior to the earthquake, although strains were probably accumulating for one hundred years.

Reid recognized two distinct phases of crustal deformation. During a period of perhaps 100 years prior to a great earthquake, slow elastic strains build up on opposite sides of the fault, essentially a couple (Fig 1A, interseismic). During this period the fault (dashed line) is assumed to be locked. When the frictional strength of the crust is exceeded, an earthquake will occur accompanied by an abrupt rebound of the crust (Fig 1A, coseismic). The coseismic movement is in an

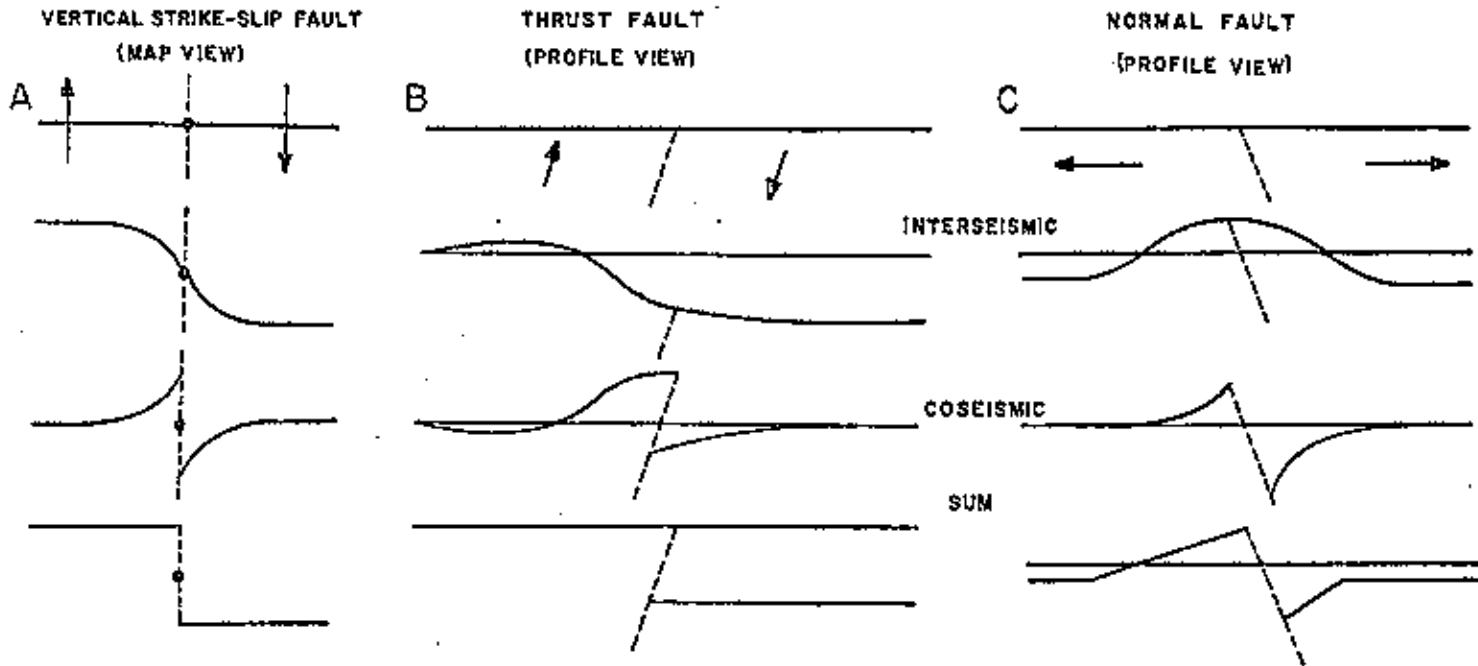
opposite sense to the interseismic strain accumulation. Summing the interseismic and coseismic movements yields the original unstrained line offset by the permanent fault displacement (Fig 1A, sum).

Similarly, an Elastic Rebound Theory consistent with thrust faulting has been proposed by Fitch and Scholz (1971) to account for ground deformations occurring before and after the magnitude 8.2 Nankaido earthquakes. Generalized in Figure 1B is a profile view of a thrust fault. Before the earthquake geodetic data suggest strain accumulated at a steady rate resulting in vertical interseismic displacements (Fig 1B, interseismic). In the 1946 Nankaido earthquake crustal deformation was produced in a direction opposite to the interseismic vertical displacements and motion was antisymmetric with respect to the fault trace (Fig 1B, coseismic, after Fitch & Scholz, 1971).

Scholz and Fitch (1969, 1970) show that, in general, interseismic movements are equivalent to movements generated by virtual slip in a direction opposite to the coseismic deformation. Evidence from the 1960 magnitude 8.5 Chilean earthquake and the 1964 magnitude 8.4 Alaskan earthquake (Plafker, 1972) suggest that the inferred mechanism of underthrusting in Southwest Japan is a reasonable model for plate interaction at island arc and arc-like structures (Fitch & Scholz, 1971).

Figure 1. Elastic rebound model of strike slip, thrust, and normal faulting. A) Strike slip faulting: horizontal deformation on a greatly exaggerated scale. Arrows show long term motion relative to the fault trace (dashed line). Interseismic curve shows formation of a couple across the fault, coseismic shows deformation produced by an earthquake, and sum is the total deformation produced by an earthquake cycle (after Reid, 1910). B) Thrust faulting: vertical scale is greatly exaggerated, arrows indicate interseismic strain accumulation in the vicinity of the fault (dashed line), while the coseismic deformation produced motion opposite to the strain accumulation. Sum shows the total of coseismic and interseismic displacements (after Fitch and Scholz, 1971). C) Normal faulting: vertical scale is greatly exaggerated. Arrows indicate long term tensile strain accumulation. Interseismic motions produce doming in the vicinity of the fault (dashed line). Coseismic rebounding produces motion opposite to the interseismic strain accumulation. Sum shows the total deformation relative to an initially level unstrained surface.

Figure 1



a

FINITE ELEMENT METHOD

The finite element method (Zienkiewicz et al., 1968) is a powerful numerical procedure which can be used for solving problems in rock mechanics. The model is composed of an interlocking set of piecewise elements, in this case triangles, that are connected at nodes, and the total of which approximates a general displacement function (Segerlind, 1976). The displacement function is approximated over each element by a polynomial that is defined using the nodal values of the displacement function. Nodal displacements are related to forces acting on the nodes through a matrix formulation dependent on the displacement function and material properties of each element (Bischke, 1974). The displacement function allows the continuum of elements to be translated, strained, or rotated in any arbitrary direction within a vertical plane. Elements are connected at common nodes and approximate the shape of the structure, and their polynomials are designated to assure that continuity is maintained along element boundaries.

Zienkiewicz et al. (1968) and Bischke (1974) described the visco-elastic procedure used here, where creep strains are calculated for a specific time interval. The creep strains are added to existing strains and solved by computer iteration according to prescribed rheologic laws.

In this case the elements behave as Maxwell bodies, i.e. springs and dashpots connected in series (Fig 2A, 2B). The spring is assumed to obey the elastic Hookean relation, $\sigma = E\epsilon$, and the dashpot is assumed to obey the viscous relation, $\sigma = \mu\dot{\epsilon}$,

where:

σ = initial stress,

ϵ = strain,

$\dot{\epsilon} = \Delta\epsilon/\Delta t$,

E = Young's Modulus,

μ = the Newtonian viscosity (See Bischke, 1974).

Thus, for a constant load, the visco-elastic strain increment is:

$$\Delta\epsilon = \sigma/E + \sigma\Delta t/\mu = \sigma(1/E + \Delta t/\mu).$$

For the lithosphere the viscous creep is suppressed by setting μ very large, approximately 10^{27} poise.

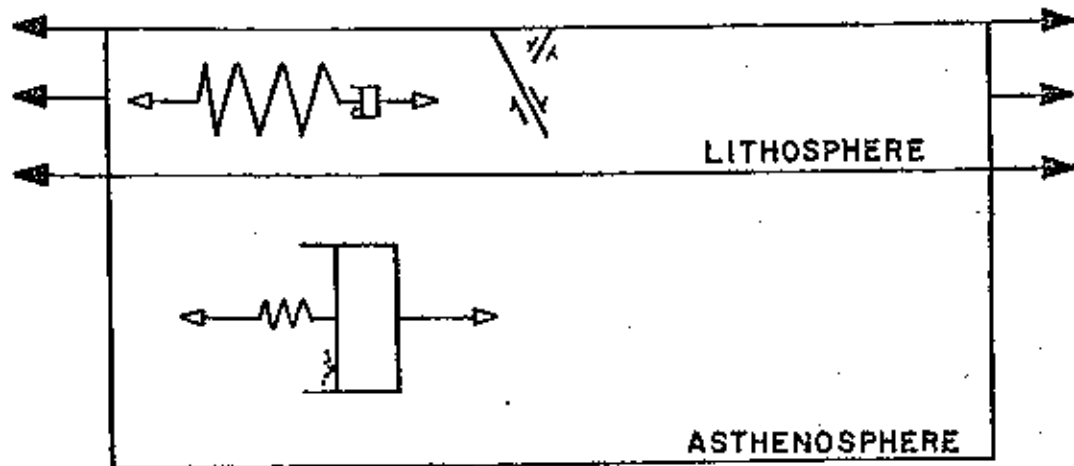
Initially the model is run for a simulated 1000 years and allowed to stabilize. The stress trajectories are then horizontal and stresses approach 30 bars in the lithosphere and less than one bar in the asthenosphere. The horizontal stresses indicate that the lithosphere is acting as a stress guide (Elasser, 1969).

The fault displacement is modeled by a method used by Bischke (1974, 1976), where the fault is represented by rectangular elements of zero thickness. This procedure is much more general than dislocation theory (Savage &

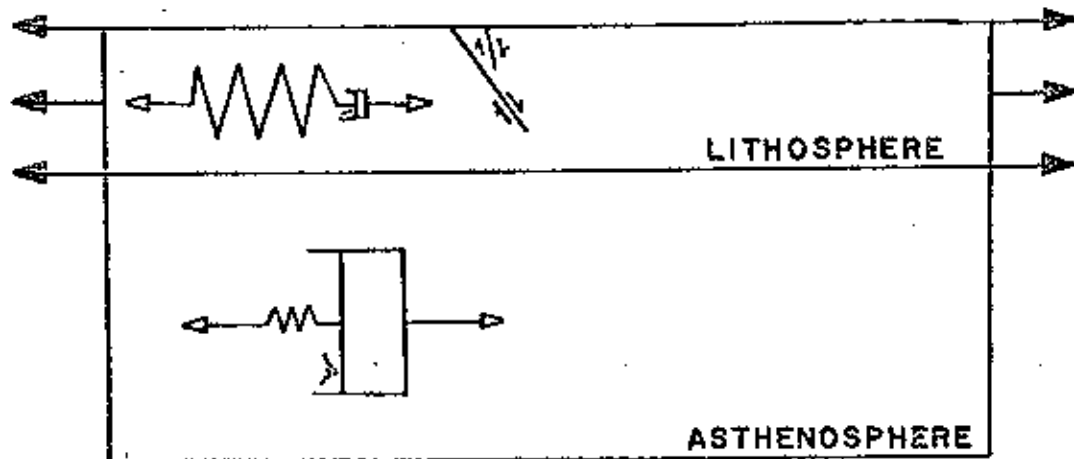
Hastie, 1966, 1969; Maruyama, 1964). However, as each Maxwell element contains an elastic response, when slip is applied to the fault surface at a time increment, $t=0$, the elastic response is similar to the dislocation models of Savage and Hastie (1966).

Figure 2. Diagrammatic cross section of the models used to generate normal fault earthquake cycles showing loading systems and generalized simple models of lithospheric and asthenospheric rheologic properties (Spring and Dashpot). Models are allowed to displace in a horizontal direction at the base. A) Fairview Peak model showing general configuration of the asymmetric graben. B) Hebgen Lake model fault configuration. Models are not drawn to scale.

Figure 2



FAIRVIEW PEAK MODEL



HEGGEN LAKE MODEL

MODEL FORMULATION

The models used for the Fairview Peak and Hebgen Lake regions are shown in Figures 1C, 2A, and 2B. The surface layer contains one or more normal faults which extend through 75% of the lithosphere. The models are 300 km in length and extend to a depth of 70 km. Model depth and length was assigned to assure that all stress changes generated by a simulated earthquake cycle were contained within the model boundaries. The model parameters are given in Table 1.

The lithosphere is defined by the effective elastic thickness assigned to the model, and was 20 km thick, based on seismic refraction measurements of Eaton (1963). The lithosphere is capable of supporting large tensile deviatoric stresses; these stresses are applied symmetrically with respect to the fault. Large loads, or stresses, produce more rapid extension. In both models, tensile loads are consistent with in situ stress measurements (Sbar & Sykes, 1971) on the order of 30 bars. During the simulated earthquake, a dislocation slip produces a stress drop in the model and causes stresses to be locally nonequilibrated, on the order of one hundred bars. The high stress drop required to model the geodetic data might suggest that these earthquakes are underdamped (Fitch & Scholz, 1971). In an underdamped situation motion during the earthquake releases more stress than has accumulated

during the interseismic period. However, there is no data available to test an underdamping hypothesis.

These models use a linear Maxwell asthenosphere described by Bischke (1974) to simulate visco-elastic conditions. The asthenosphere is generally 2-3 times the lithosphere thickness to insure that the model extends deeper than the crustal compensation depth. The base of the model is allowed to displace in a horizontal direction but not in a vertical direction. Interseismic creep strains are generated in response to the non-equilibrated stresses caused by the dislocation slip (Bischke, 1976). The rate at which interseismic strains accumulate is primarily dependent upon the viscosity of the asthenosphere.

Table 1. Values Used in the Best Fit Finite Element Models.

Fairview Peak Model

Layer	Layer Thickness (km)	Young's Modulus ($\times 10^6$) Bars	Poisson's Ratio	Effective Newtonian Viscosity, P
Lithosphere	20	0.88	0.26	3.0×10^{27}
Asthenosphere	50	0.88	0.40	2.1×10^{21}
Fault Depth	6 km			
Fault Slip	1.9 m			

Hebgen Lake Model

Layer	Layer Thickness (km)	Young's Modulus ($\times 10^6$) Bars	Poisson's Ratio	Effective Newtonian Viscosity, P
Lithosphere	20	0.88	0.26	3.0×10^{27}
Asthenosphere	50	0.88	0.40	2.3×10^{21}
Fault Depth	12 km			
Fault Slip	6.0 m			

MODEL RESULTS

The results obtained from model studies are fundamental to the understanding of crustal deformation in divergent zones. Hundreds of models were run with different loading systems and varying elastic and viscous constraints; all results were similar to Figure 1C.

Block faulted and rift zones are systems of dip slip or normal faults which form perpendicular to regional tensile stress (Hobb et al., 1976). They usually comprise the youngest structures in many regions (Hobb et al., 1976). In this thesis the finite element method is used to formulate an elastic rebound theory for rock subject to tensile stresses. During the interseismic period before a large earthquake, tensile deviatoric stresses are applied to a modeled elastic lithosphere, which accumulate in the vicinity of the fault. A perfectly elastic slab will deform similar to Figure 1C (interseismic). In the case where block faulting predominates, the secular deformation will be expressed by a doming of the crustal blocks in the vicinity of the fault zone. The only case where there was no pattern of interseismic doming was during model runs when the dislocation slip fractured through the lithosphere. Ground displacements generated for areas of normal faulting will show relative changes in elevation because geodetic data are not well constrained to an absolute base level (i.e. point of no

vertical motion). When the frictional strength of the crust is exceeded the crust will rebound in a direction opposite to the displacement which occurred during the strain accumulation phase (Fig 1C, coseismic). The coseismic phase generated in this model is similar to the dislocation models of Savage and Hastie (1969).

In actual situations uplift (Fig 1C) is less than predicted from the model. This may be due to the effect of consolidation or compaction of the uplift zone, survey error, or possibly due to the effect of the fault intersecting a free surface. Furthermore, survey data is based on relative changes in elevation, relative to some point far removed from the deformed area, which is assumed to have remained stable or fixed between surveys. However, fixed points of the survey may have moved considerably between measurements. Thus, only relative changes are significant.

Interseismic and coseismic movements result in no net strain accumulation and a permanent displacement along the fault (Fig 1C, sum). The footwall portion forms a horst while the hanging wall is downwarped in the vicinity of the fault. Thus an elastic rebound model seems reasonable in regions where the plates diverge, or are subject to crustal extension. Continued normal faulting and strain accumulation should produce a topography of great relief, including narrow linear mountains (horsts) with intervening valleys (grabens).

GEOLOGY, SEISMICITY, AND TECTONICS OF THE FAIRVIEW PEAK,
NEVADA AND HEBGEN LAKE, MONTANA REGIONS

The epicentral area for the Fairview Peak earthquake lies within the Basin and Range Province (Fig 3). The area is presently subject to crustal extension with an average rate of extension of at least 0.4 mm/yr for the past 15 million years (Thompson & Burke, 1973). Extension rates may be as high as 0.3-1.5 cm/yr (Stewart, 1971). The microseismicity and tectonics of the Nevada seismic zones (Gumper & Scholz, 1971) reveal a narrow, but major zone of seismic activity producing NW-SE crustal extension. This agrees well with historic faulting in the area (Byerly, 1956).

The Basin and Range Province consists of linear mountains with intervening alluviated valleys. The maximum relief is approximately 2 km and is supported by a 25 km crust (Bott, 1971). The area is isostatically compensated as a whole, although local positive and negative anomalies are apparent over mountains and valleys, respectively (Thompson, 1959). The Province is bordered on the east by the Colorado Plateau and is abruptly terminated in the west by the Sierra Nevada Batholith (Smith, 1973).

The Basin and Range Province has many features similar to active rifts and interarc basins. This area has a thin crust, 20-30 km (Prodehl, 1970), and high heat

flow, $\approx 2.0 \mu\text{cal}/\text{cm}^2 \text{ sec}$ (Roy et al., 1968), and low crustal and upper mantle P and S wave velocities (Pakiser & Zietz, 1965). Molnar and Oliver (1969) have shown that high frequency Sn phase is highly attenuated across the province, a characteristic of mid-ocean ridges and regions behind island arcs (Karig, 1971a).

During the Mid-Tertiary normal faulting began in the Hebgen Lake, Yellowstone region (Fig 3). The tectonic development of this area is similar to the Basin and Range Province (Trimble & Smith, 1975). The intermountain seismic belt, including Hebgen Lake, extends from Utah northward through Montana (Sbar et al., 1972), and is characterized by east-west tensional stress coincident with a north trending zone of normal faults (Smith & Sbar, 1974). The zone is intersected in the vicinity of Hebgen Lake by the Idaho seismic zone, a north-south tensional zone (Trimble & Smith, 1975).

Hamilton and Myers (1966) suggest that the Snake River Plain to the south of the Hebgen Lake area (Fig 3), covered by Pliocene and Quaternary basalt flows, may represent a lava filled tensional rift. Cenozoic silicic volcanism in the Great Basin (Armstrong et al., 1969) may have a similar mechanism, paralleling the expansion of normal faulting. Morgan (1972) has suggested that the Snake River Plain may be the result of the North American

plate overriding a hot spot. Similarly Armstrong et al. (1969) suggest a primary motivating force in the mantle for volcanism in the Great Basin. The spatial relation of the Idaho Batholith to the Hebgen Lake region and the Sierra Nevada Batholith to the Fairview Peak region (Fig 3) suggests greater complexities than a simple primary force within the mantle or simple plate motion over a hot spot. The similarity of the Fairview Peak and Hebgen Lake regions to active rifts and interarc basins is possibly an expression of the North American plate overriding the subducted East Pacific Rise (Scholz et al., 1971).

Figure 3. Tectonic setting of the western United States.

Fairview Peak, Nevada is shown with the approximate position of USCGS precise level line along US 50. Lines in the Basin and Range Province represent major faults. Hebgen Lake, Montana is shown with the approximate position of USCGS precise level lines used for the interseismic deformation (See Fig. 13). Line AB represents a USCGS level from Idaho Falls (A) to West Yellowstone (BM N-33) (B). Line BC extends from BM N-33 (B) to Bozeman (C) (after Sbar et al., 1972; Reilinger et al., 1977).

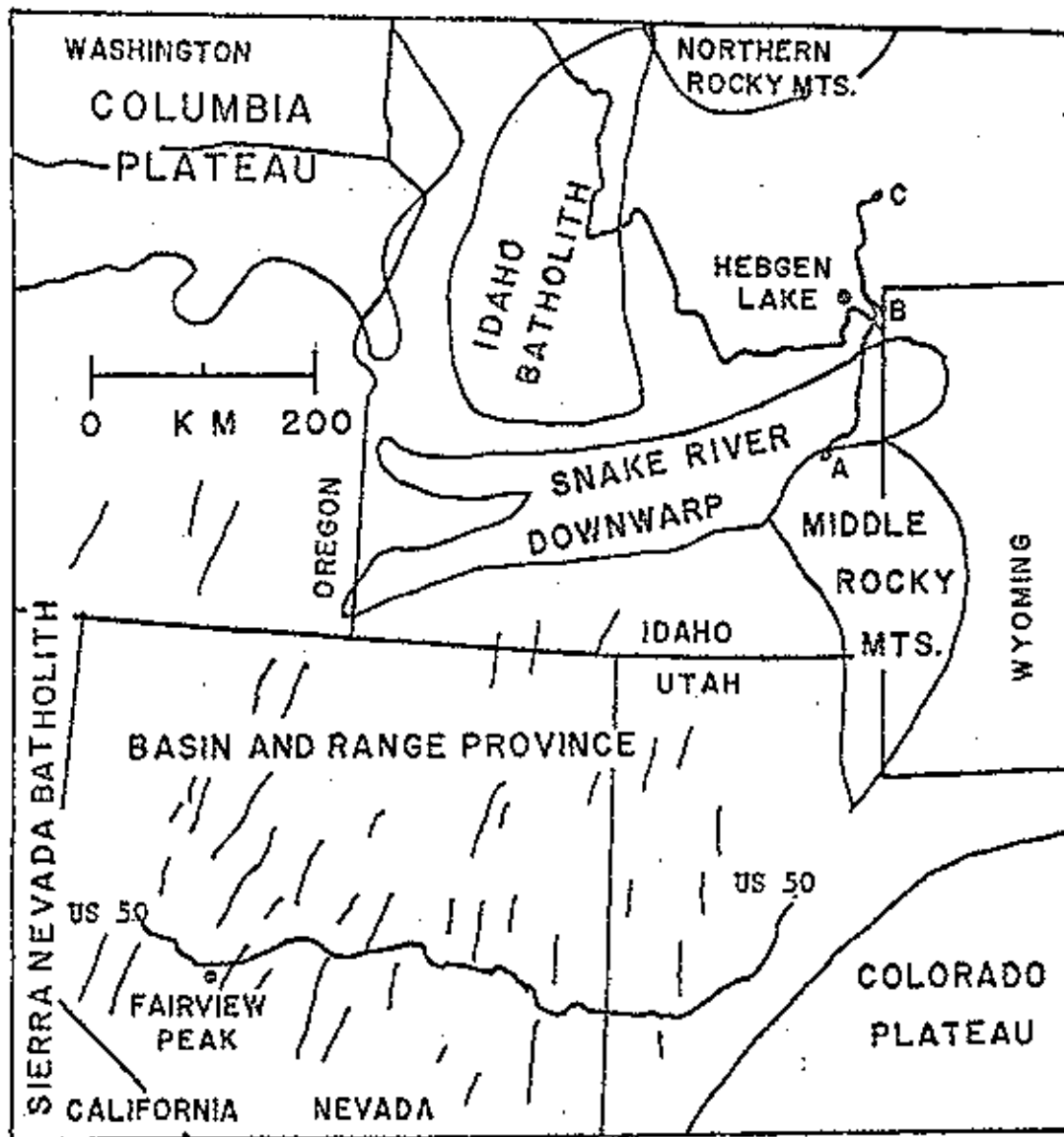


Figure 3

SURVEY DATA

Elevation changes are obtained by subtracting the observed elevation difference between a reference benchmark and some given benchmark, and redetermining that difference at some later time. This is only a relative elevation change not connected to any absolute reference; thus, absolute elevation changes are not known. Survey errors present the greatest difficulty in evaluating elevation changes. Errors may arise from survey mistakes, systematic errors, or from random survey errors (Brown & Oliver, 1976).

USCGS surveys, designated first order level, are double run surveys. Measurements of elevation changes are performed twice: once from benchmark (BM) -A to BM-B, and once from BM-B to BM-A (Brown and Oliver, 1976). This determination of elevation change gives an estimate of the precision of the survey and also reduces or eliminates the effects of survey mistakes. USCGS surveys, designated second order level, are generally run over shorter distances than first order level surveys and are often not double run surveys.

Systematic errors are the most serious type of survey errors. They occur usually with the same sign and accumulate over a distance (Brown & Oliver, 1976). First order level surveys are designed to eliminate or reduce systematic errors. However, there is no proof that the

double run procedure cancels this effect (Savage & Church, 1974).

Random survey error can be expressed as the square root of the distance measured (L) (Brown & Oliver, 1976). The standard deviation for random survey error is given by the relation, $\sigma = ML^{\frac{1}{2}}$, where σ is the standard deviation of elevation difference in mm, determined over the distance L in km. M is the standard closure of a double run section (Bomford, 1971). M is estimated for the survey intervals by Holdahl (1973a) as 1.5 mm for the time period 1917-1955, and 1.0 mm from 1956 to the present. These values are used to calculate random error in the data interpreted here.

Fairview Peak, Nevada Geodetic Data

Coseismic

In 1934, the USCGS established a vertical level line running from Coinville, Utah to Hazen, Nevada along US Highway 50 (Fig 3). On December 16, 1954 two strong earthquakes struck the Basin and Range Province with their epicenters in west-central Nevada (Fig 4). The Fairview Peak earthquake caused displacements on a normal fault (Romney, 1957) perpendicular to and crossing Highway 50, 5 km west of West Gate, Nevada. Both horizontal and vertical components of equal magnitude were indicated by the seismic solution. Geodetic studies substantiate the focal mechanism solution and reveal a maximum strike

Figure 4. 1954 Nevada earthquakes showing relative vertical motion. Epicenters are shown by open circles (after Richter, 1958).

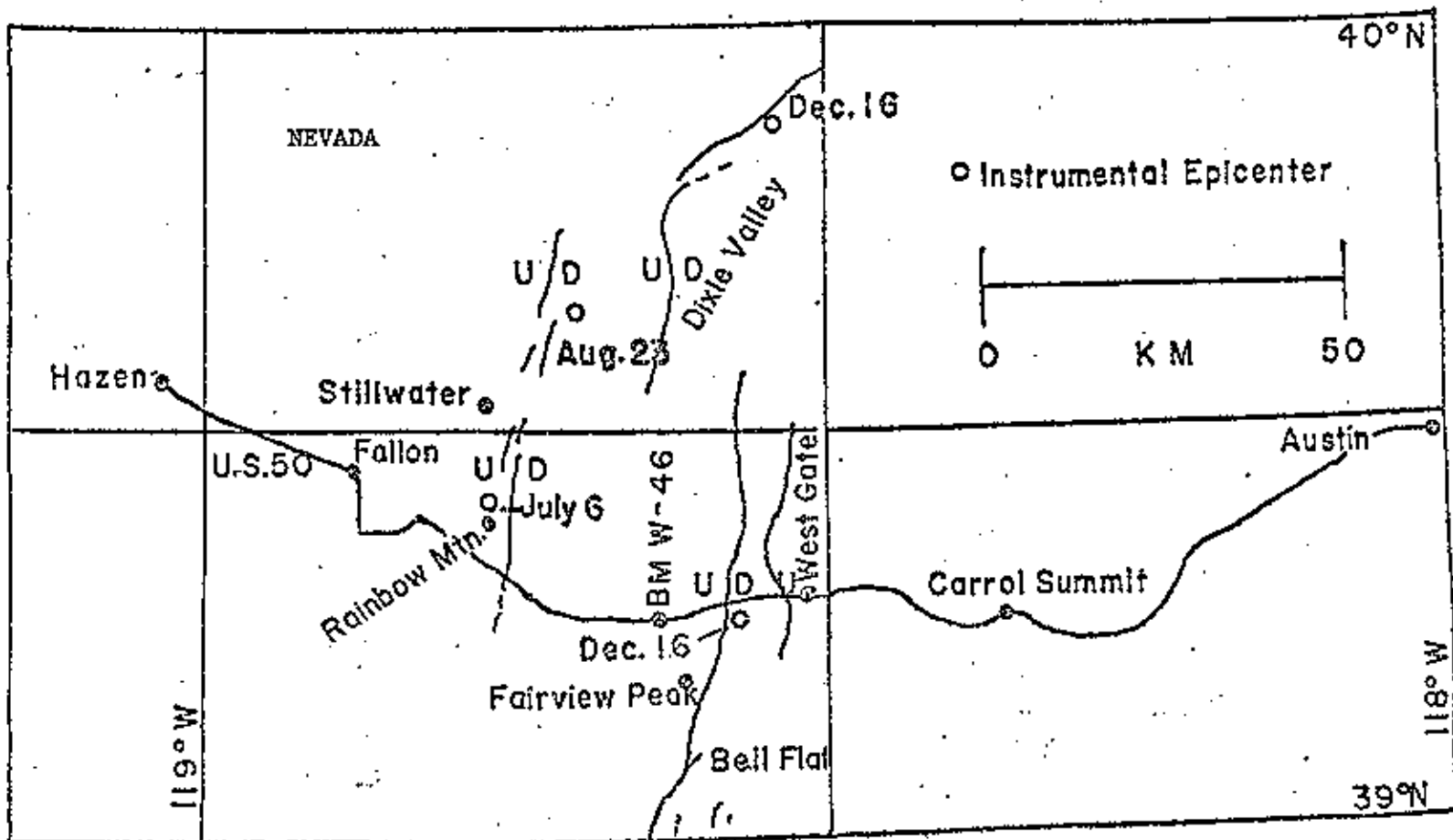


Figure 4

slip component of 3.5 meters at Fairview Peak and a maximum vertical displacement of 3.5 meters at Bell Flat (Slemmons, 1957).

Coseismic displacements were confirmed by a USCGS level run along Highway 50 in 1955 (Fig 6). The deformation and ground breakage has been discussed by Savage and Hastie (1966, 1969), Meister et al. (1968), and Whitten (1957). The Nevada Highway Department (Reil, 1957) also ran a level along Highway 50 after the 1934 USCGS survey, and again one month after the earthquake. These ground displacements are likely to contain less interseismic strain accumulation, thus better depicting the coseismic phase (Fig 5A).

Figure 6 shows the change in elevation between 1934-1955 revealed by USCGS first order level lines. The most obvious feature is the coseismic deformation which occurred along the Rainbow Mountain and Fairview Peak faults. West of Fairview Peak three earthquakes occurred within six months of the Fairview Peak earthquake. The surface faults are shown in Figure 4. It is likely that these earthquakes caused considerable movement affecting the USCGS level along Highway 50 west of Fairview Peak. The lack of compensating coseismic uplift at Fairview Peak could be caused by downward fault movement west of Fairview Peak. Moreover, during the earthquake the footwall is extended causing uplift of the footwall and

Figure 5. A) Coseismic vertical deformation as revealed by the Nevada Highway Department. Elevation changes are relative to BM N-46 (after Reil, 1957).
B) The coseismic vertical deformation of the Fairview Peak model from selected surface nodal points which was produced by 1.9 m of uniform dip slip motion extending to a depth of 6 km.

Figure 5

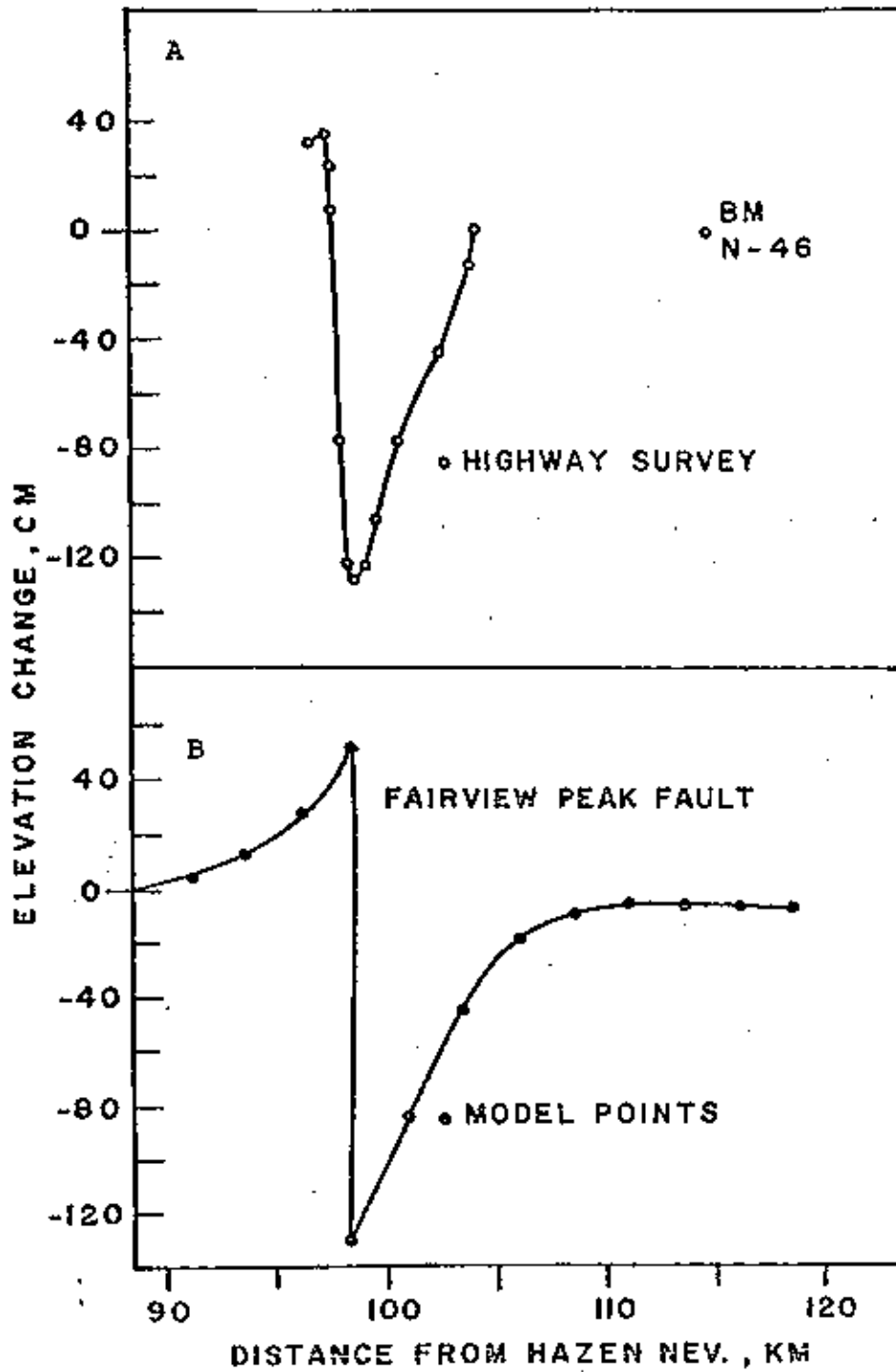
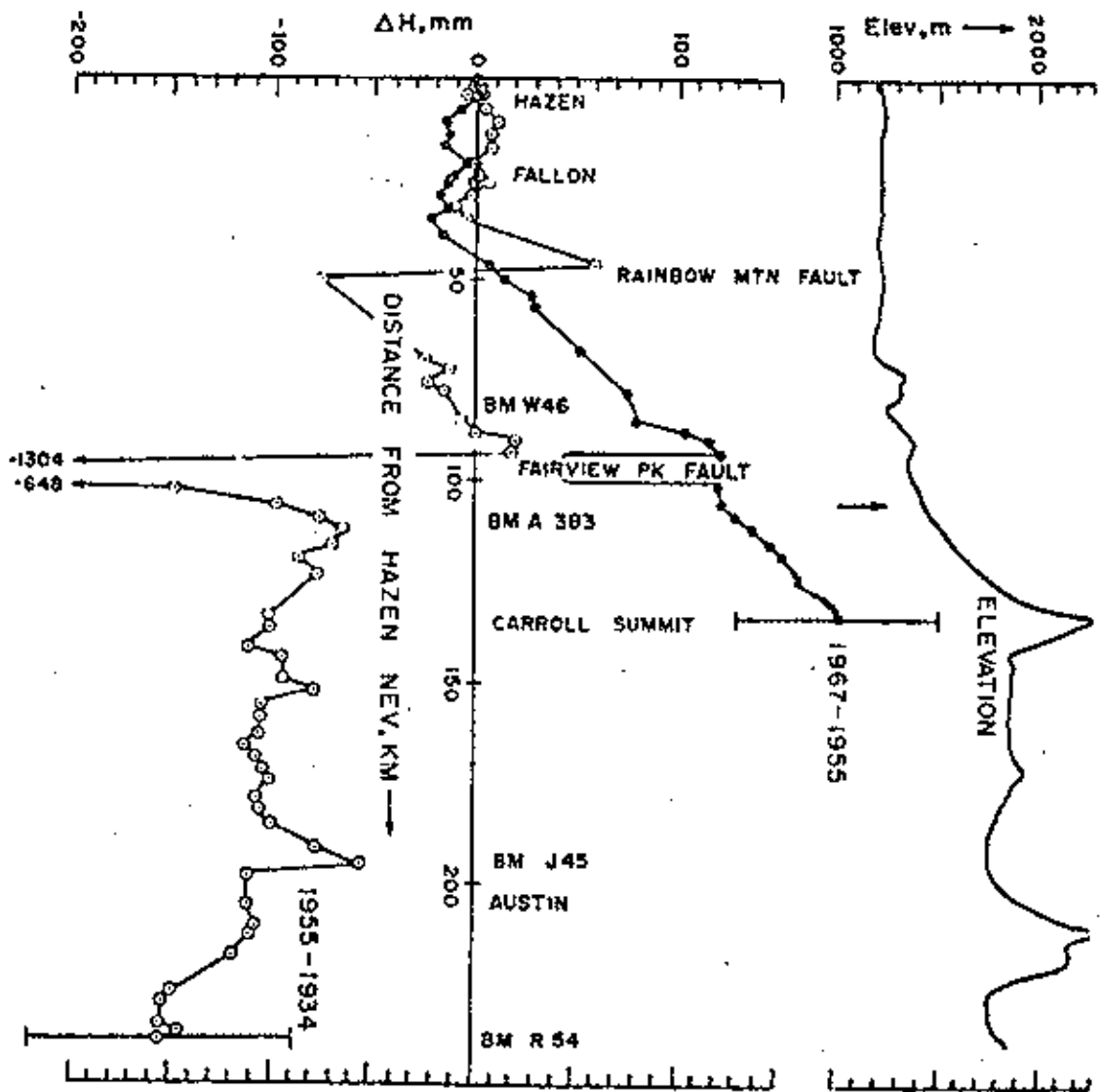


Figure 6. Elevation changes of USCGS levels along US 50 from 1934-1955 (open circles) and from 1955-1967 (solid circles) relative to BM B-48 Hazen, Nevada of unadjusted survey data. Error bars are shown at the right of each survey. Topographic profile is shown at the top. (From Savage and Church, 1974)

Figure 6



conclusions concerning the absence of observed extension of the footwall are problematic. Similarly any inter-seismic or post-seismic strain accumulation and/or release would also affect the survey data (Fig 6). The overall trend of the 1934-1955 elevation changes is about 0.8 mm/km tilt to the east (Fig 6; after Savage & Church, 1974). The tilt is greater than random survey error, and suggests that the area to the east of Fairview Peak was depressed prior to the earthquake. Such a depression would be expected from the rebound model for normal faults (Fig 1C).

Post-Seismic

The USCGS in 1967 resurveyed a 90 km section of Highway 50 crossing Fairview Peak (Fig 6). There is evidence for local slip across five fault scarps which faulted in 1954 (Savage and Church, 1974). The most obvious feature of the survey is the 2.0 mm/km tilt to the west (Fig 6,7).

Savage and Church (1974) examined the misclosures for the 1967 first order level, which gives an estimate of the precision of the level. Usually misclosures are random, but in the 1967 survey they were not, and accumulated nearly linearly with distance. Savage and Church (1974) estimate a 104.6 mm systematic error at the 95% confidence level. This error is nearly the same magnitude as the

observed tilt. Furthermore, there is a high correlation between tilting and elevation. This suggests other systematic errors, such as rarefraction (Brown & Oliver, 1976; Savage & Church, 1974).

A rare combination of oscillations in crustal deformation would be required for the 1967 survey data to be valid, such as continued slip on the 1954 faults to produce slip anomalies, backslip at depth to produce tilting of 2.0 mm/km to the west, and interseismic tilting of at least 3.2 mm/km to the east. Furthermore, some interseismic deformation must have occurred between 1955-1967.

Admittedly oscillations of crustal deformation of these types and magnitude have been observed for many earthquakes (Scholz & Kato, 1978; Scholz, 1972; Savage & Church, 1974). However, rapid crustal oscillations of the type inferred from the 1967 survey, if modeled, would require high tensile deviatoric stresses, on the order of 1000 bars, producing high rates of extension, greater than 5 cm/yr. Extension rates of this magnitude are not observed (e.g. Thompson & Burke, 1973; Stewart, 1971), and tensile stresses of 1000 bars are unlikely compared to in situ stress measurements of 30 bars tensile stress east of the Basin and Range Province in the intermountain seismic belt (Sbar & Sykes, 1973). Thus, it appears probable that the 1967 survey is contaminated by systematic

error.

Interseismic

As part of a premonitory earthquake program the USCGS resurveyed a 35 km section of Highway 50 crossing Fairview Peak in 1973. The survey shows no anomaly of local slip across the Fairview Peak fault but does show a 1.7 mm/km tilt to the east between 1967 and 1973 (Fig 7, after Savage & Church, 1974). If the 1967 survey was contaminated by systematic error and there was no change in elevation between 1967 and 1973, Figure 7 (1967-1973) could be reproduced. It is unlikely in view of the large systematic error in the 1967 survey that the change in elevation between 1967 and 1973 is due to actual crustal movement.

The 1955-1973 elevation changes provide the best estimate of the interseismic deformation occurring across the Fairview Peak fault (Fig 7, 1955-1973). Again there is evidence for continued slip at Fairview Peak, although there is no other significant trend. This suggests that the interseismic crustal movements are occurring at a slow rate without rapid regional tilting and that the post-seismic movements did not continue past 1967.

Figure 7. USCGS elevation changes relative to BM W-46 indicated by the 1955, 1967, 1973 surveys (after Savage and Church, 1974).

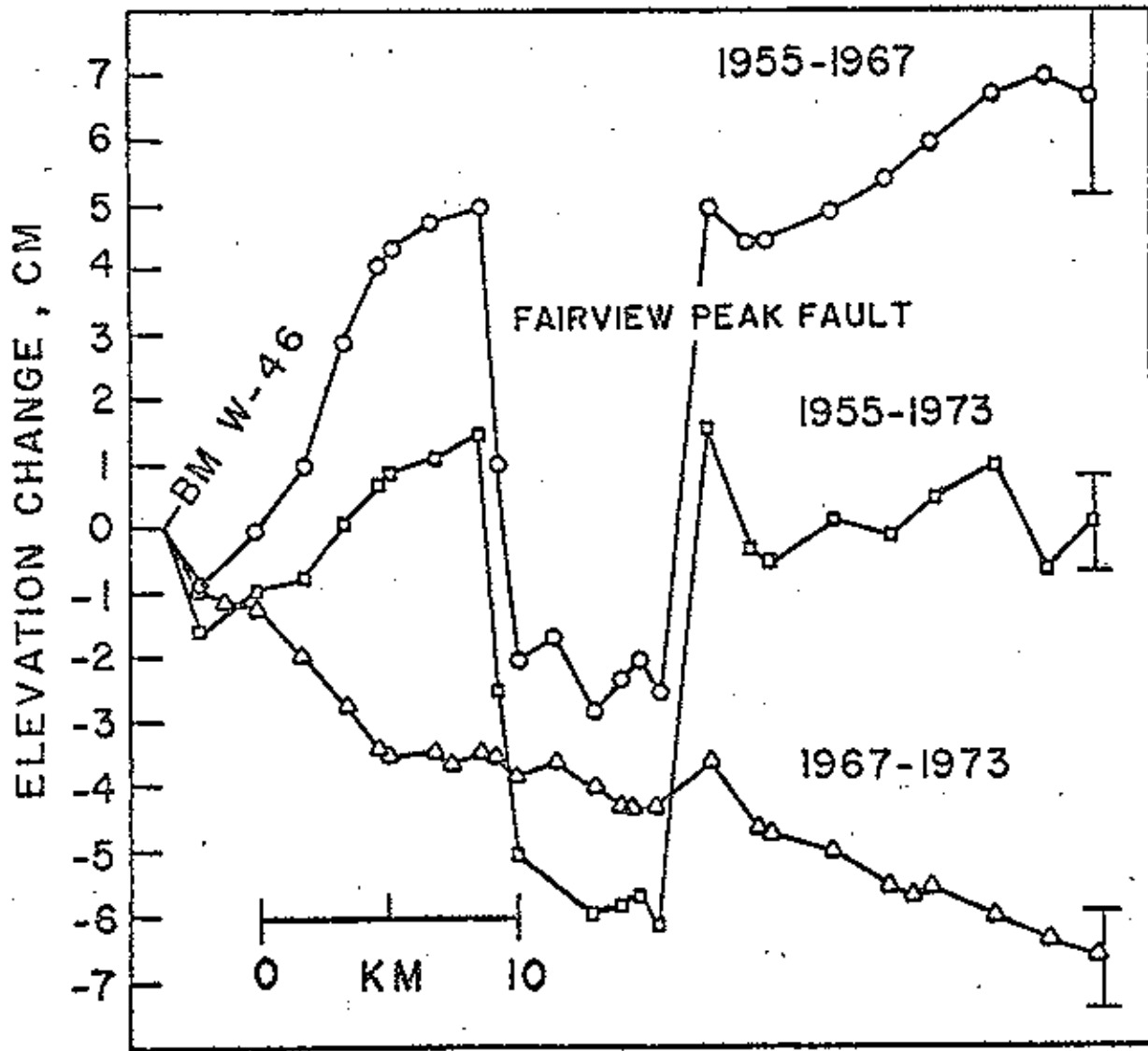


Figure 7

FAIRVIEW PEAK MODEL

The Fairview Peak model consists of a 20 km lithosphere overlying a 50 km asthenosphere. The base of the model does not coincide with the base of the asthenosphere, which is presumably at greater depth. However, all earthquake stress changes simulated by the model are confined to the model boundaries.

The Fairview Peak field data (Slemmons, 1957; Whitten, 1957) suggest the formation of a graben between Fairview Peak and West Gate, Nevada (Fig 4). Stewart (1971) suggested that many of the valleys within the Basin and Range Province are asymmetric grabens, marked on one side of the valley by a master fault. The other side contains a minor fault dipping towards the master fault (Fig. 2A). The Fairview Peak fault is modeled as the master fault, from the seismic solution of Romney (1957), indicating a fault striking $N 11^{\circ}W$ and dipping $62^{\circ}E$. During the simulated earthquake the minor fault was not allowed to slip. The focal depth from the seismic solution is about 15 km (Romney, 1957).

Fault slip (i.e. an earthquake) is produced by applying a displacement dislocation across selected fault elements (Bischke, 1974). Fault slip was estimated from geodetic resurvey (Fig. 6, 1934-1955) to be approximately 130 cm of downward displacement and 20 cm of corresponding uplift; however, best fit model generated uplift is on the order of 50 cm (Fig. 5B).

Dislocation models of Savage and Hastie (1966) suggest that the 1.5 m dip slip displacement revealed by the geodetic survey levels extended to a depth of about 5 km. This is about 1/3 the depth indicated by the focal mechanism solution of Romney (1957). This does not mean that faulting ceased at 5 km; it is thought that during some earthquakes a decrease in slip in the down dip direction is a more accurate representation of faulting (Fitch and Scholz, 1971). In the model used here, induced faulting extends to a depth of 5-6 km. Below this depth the fault can sustain a shear stress of about 10^7 bars without slippage. The coseismic model generated results presented here are very similar to the dislocation model results of Savage and Hastie (1966).

Figure 5A and 5B show a comparison of the Nevada Highway Department leveling data and model generated points for the Fairview Peak coseismic phase. The model solution is primarily dependent on the amount of slip applied to the fault and the depth of the slip dislocation. Variations of model parameters, such as loads and elastic constants, had little influence on surface generated points and simulated earthquake generated stress changes. The close agreement between model generated points and the highway survey supports the concept of a lithosphere subject to elastic rebounding, and corroborates well with the dislocation models of Savage and Hastie (1966).

According to Brune and Allen (1967) The Fairview Peak earthquake produced a seismic stress drop of 180 bars. This is an unusually large amount of stress release as compared to 30-70 bar stress drop observed at convergent plate margins (Kanimori & Anderson, 1975). Model results produce a stress drop of approximately 80 bars maximum (Fig 8). However, only vertical displacements were used to generate the stress drop in the model and vertical and horizontal displacements were nearly equal (Slemmons, 1957). As shown in Figure 8, the major shear stress drop in the Fairview Peak earthquake model occurs below the footwall portion of the fault. The hanging wall block is highly compressed near the end of the fault resulting in a stress increase of 100 bars. Furthermore, small stress changes extend to a depth of 50 km, although all stress drops greater than 5 bars were confined to the modeled lithosphere.

A stress recovery map (Fig 9) assuming the fault is locked between earthquakes, shows where shear stress recovery is the greatest for a one hundred year period after the modeled earthquake. Portions of the lithosphere that were compressed during the modeled earthquake are relaxed, and similarly regions which experienced extension are compressed.

Figure 10 shows a model run, utilizing continued slip extending to a depth of 4 km, on two faults back to back (i.e. an asymmetric graben; Fig 2A) to produce results

Figure 8. Shear stress change parallel to the Fairview Peak model fault surface generated by a simulated earthquake. Contours indicate the amount of shear stress change in bars; stress drops are negative.

Figure 8

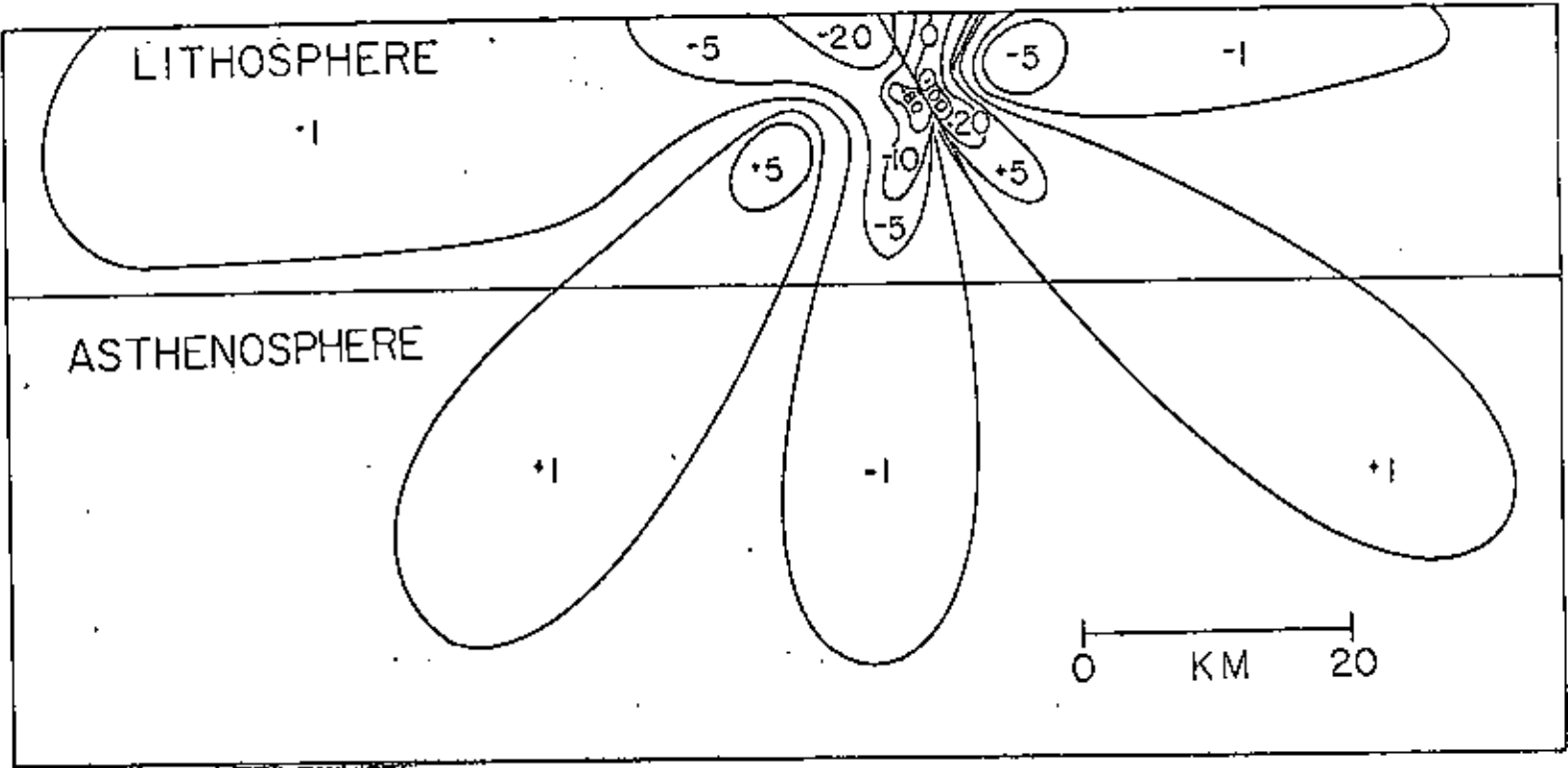
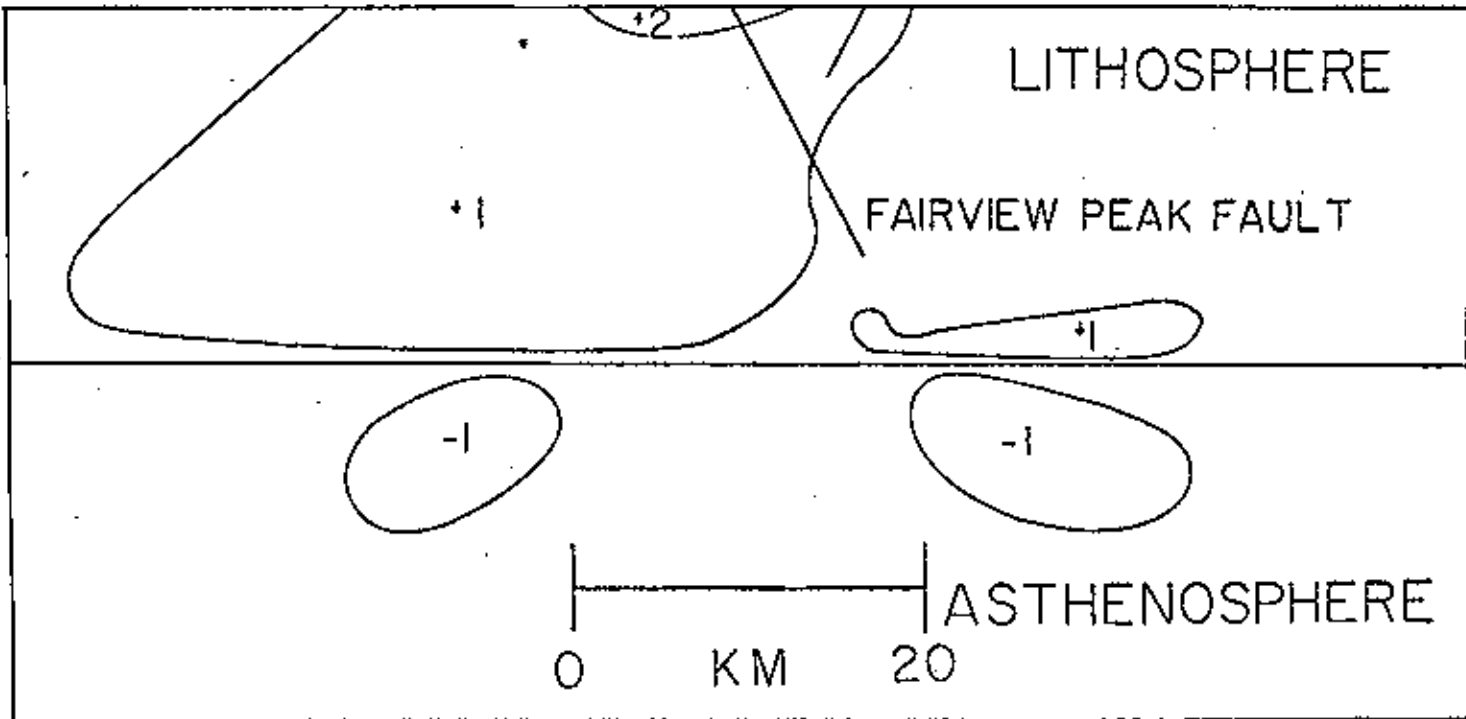


Figure 9. Amount of shear stress recovery in bars for a one hundred year period following the Fairview Peak model earthquake. See figure 8 for explanation of contours.

Figure 9

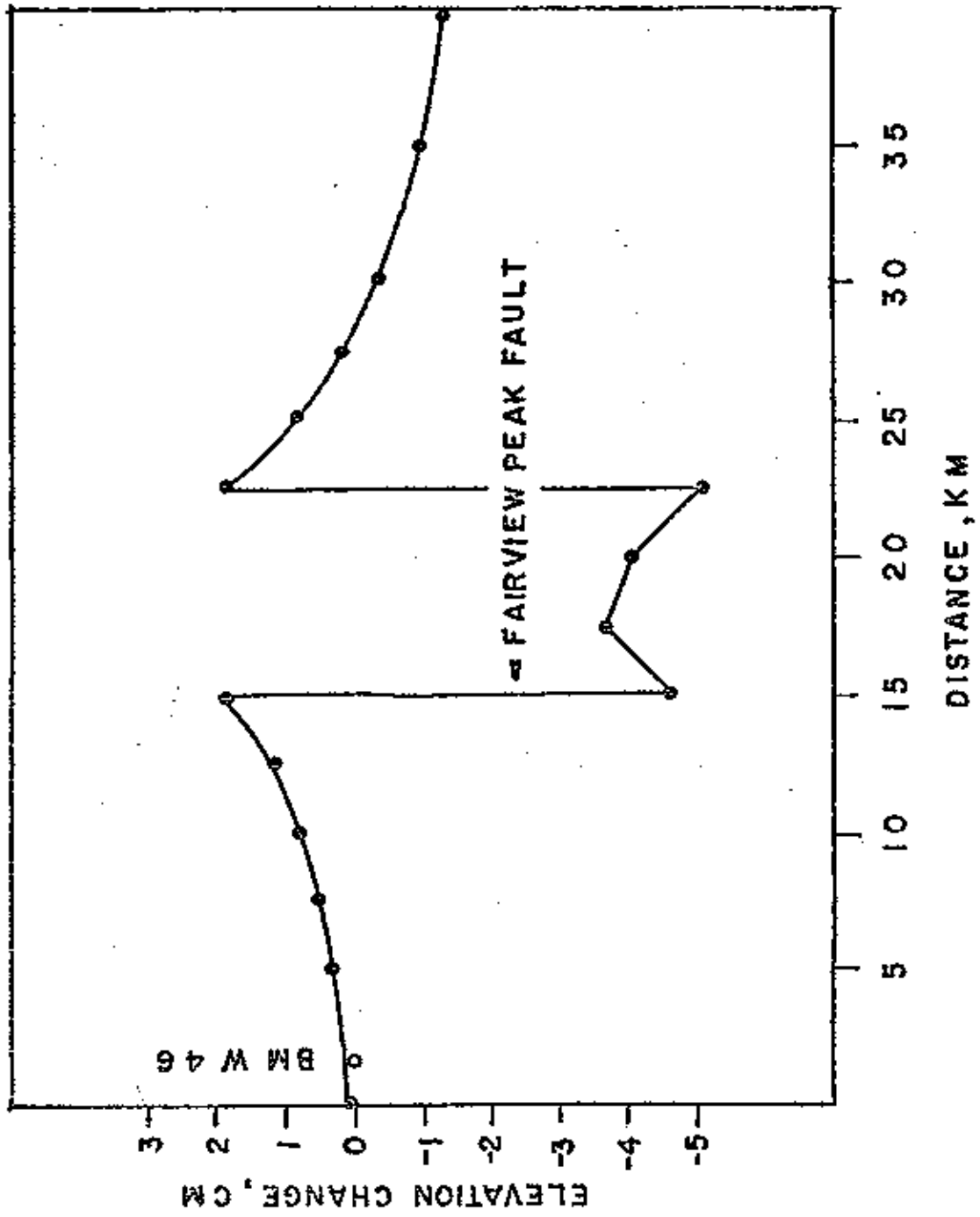


similar to the 1955-1973 elevation changes (Fig 7). Since the 1955-1973 USCGS data (Fig 7) indicates no significant trend it is not yet possible to evaluate the hypothesis of interseismic doming across the Fairview Peak fault. The data does suggest that if doming is occurring across Fairview Peak it is occurring at a very slow rate.

After a modeled earthquake the crust domes in the vicinity of the fault; the rate of doming being dependent on the asthenosphere viscosity. The viscosity inferred from the geodetic data and assigned to the model asthenosphere is within the limits quoted by Cathles (1975), i.e. 1.75×10^{21} to 2.4×10^{21} poise. A viscosity of 2.1×10^{21} poise would produce doming on the order of 0.5 mm/yr, and would only amount to about 2 cm maximum elevation change for a 20 year period following the modeled earthquake. The survey data from 1955-1973 indicates no significant trend ± 1 cm. The other alternative for lack of doming across the area suggested by the model is that faulting extended through the lithosphere. However, model studies (e.g. Savage & Hastie, 1966) suggest that most of the slip during the earthquake extended to a depth of only 5 km and the lithosphere thickness is about 20 km (Eaton, 1963). Thus it appears probable that stresses are being stored at a very slow rate across the Fairview Peak fault.

Figure 10. Model generated surface deformation including approximately 10 cm of continued slip on the Fairview Peak asymmetric graben faults, plus 18 years of strain accumulation following the modeled earthquake.

Figure 10



HEBGEN LAKE, MONTANA GEODETIC DATA

Coseismic

The coseismic deformation produced by the 1959 Hebgen Lake, Montana earthquake is discussed in detail by Myers and Hamilton (1964), Fraser et al. (1964), and Savage and Hastie (1966). The data are comprised of elevation changes detected by USCGS surveys in 1934 and releveled in 1960; data may contain some interseismic strains and post-seismic deformation. Figure 11 shows a cross section taken approximately perpendicular to the strike of faults produced by the earthquake, from USCGS composite levels (Myers & Hamilton, 1964). The data consists of first and second order levels interconnected to form a subsidence contour map. Since the data is not comprised of individual level sections it may contain some error.

Interseismic

Recent vertical crustal movements from precise leveling data (Reilinger et al., 1977) reveal a contemporary doming of an 8000 km² area including the epicentral area of the Hebgen Lake earthquake. The levelings consist of individual profile segments pieced together, and data quality, for this reason, is believed to be less reliable. Second order level lines for this data are shown in Figure 13. Figure 13 is a profile view taken approximately perpendicular to the strike of the Red Canyon and Hebgen faults (Fig 2B,12) excluding any coseismic deformation (Reilinger et al., 1977).

This doming may result from interseismic strain accumulations. Furthermore, the interseismic data consists of two levels joined at BM N-33 (Fig 13). All velocities are relative to BM N-33 which was arbitrarily assigned a velocity of 5 mm/yr, thus only relative changes are significant.

Figure 11. Vertical profile along AB in figure 12, of the coseismic deformation associated with the Hebgen Lake earthquake as revealed by USCGS elevation changes between 1934-1959 (after Myers and Hamilton, 1964). Dashed line indicates where deformation is less certain.

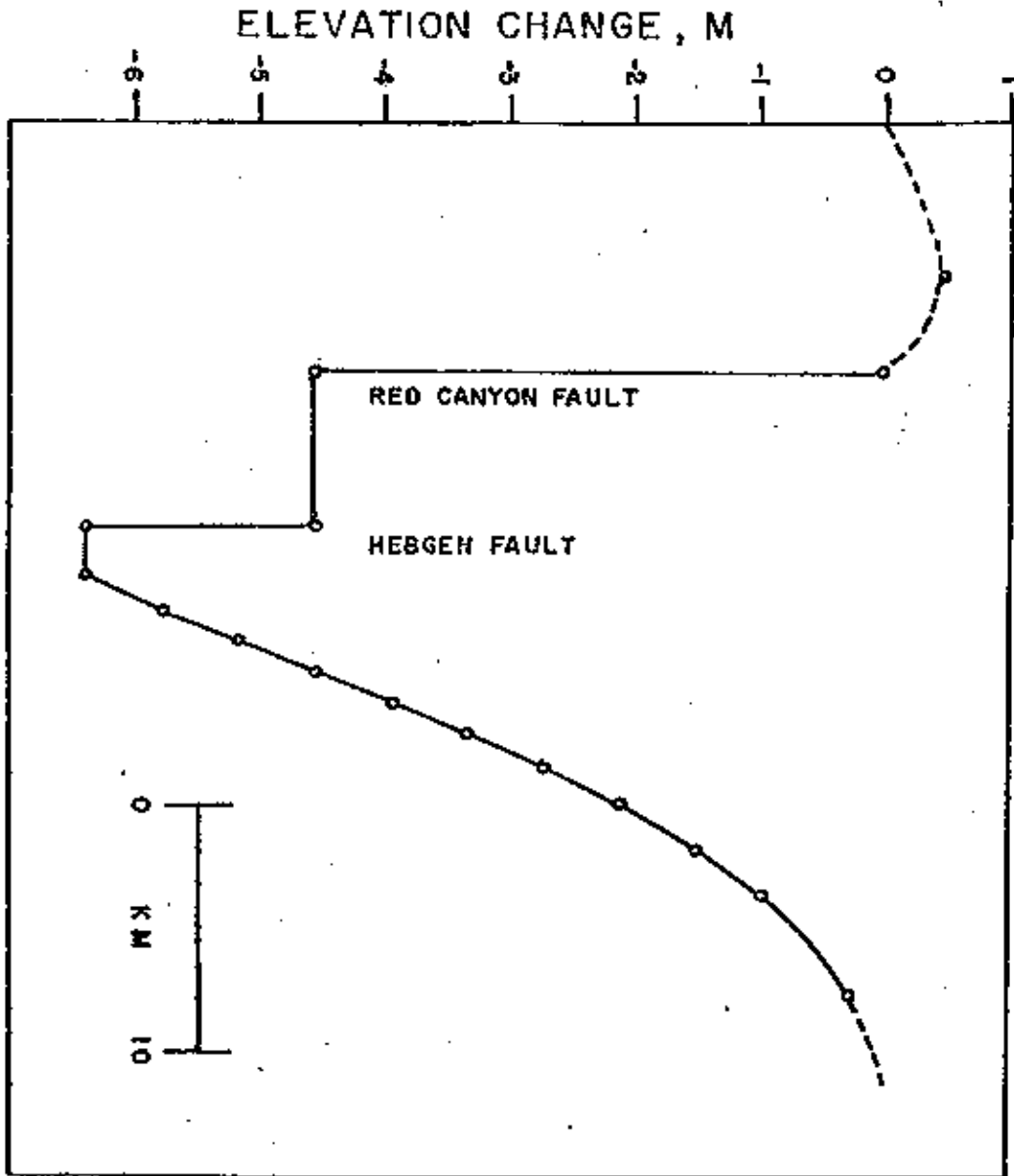


Figure 11

Figure 12. Map showing the Hebgen Lake region and position of the Red Canyon and Hebgen fault scarps. Line AB represents the approximate plane of the Hebgen Lake model (See Fig. 3; after Myers and Hamilton, 1964).

Figure 12

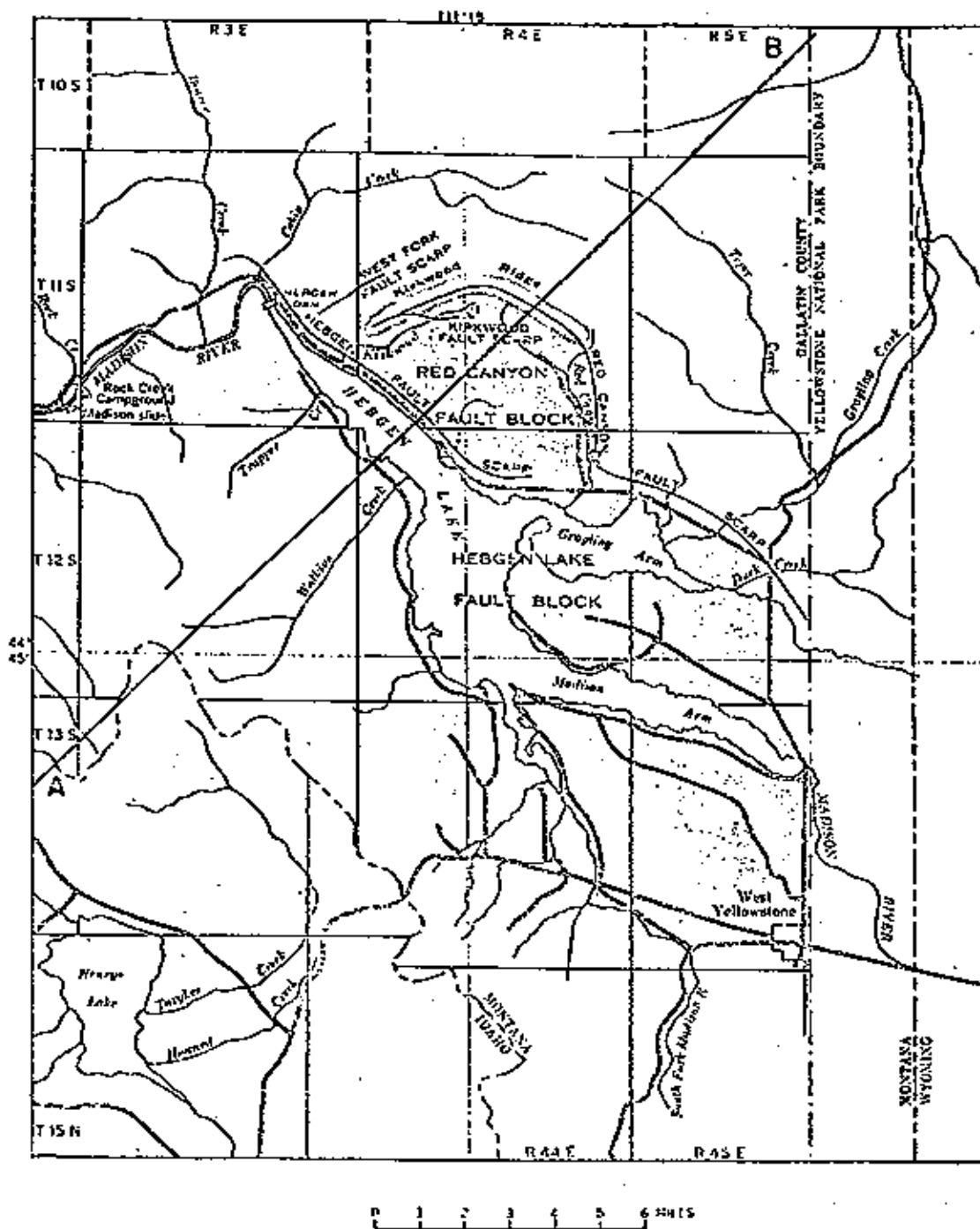


Figure 13. Interseismic strain accumulation in the vicinity of Hebgen Lake excluding any coseismic deformation. Composite of two USCGS vertical levels from Idaho Falls (A) to BM N-33 (B) and from BM N-33 (B) to Bozeman (C) (See Fig. 3). Error bars are shown at the right for level AB and at the left for level BC. (after Reilinger et al., 1977)

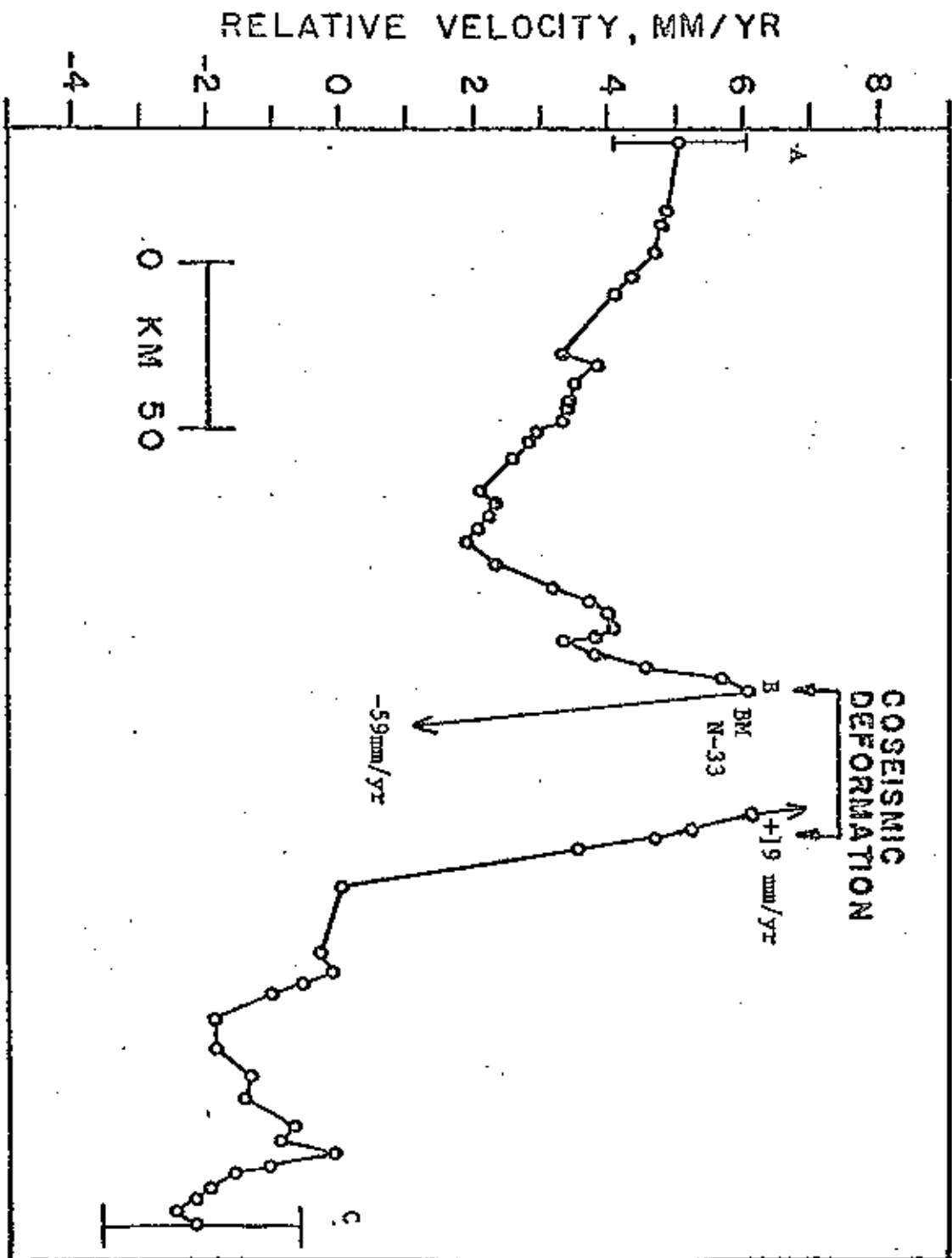


Figure 13

HEBGEN LAKE MODEL

The model consists of two faults (Fig 2B); the Red Canyon fault which produced a 4.5 meter scarp and the Hebgen fault which produced a 1.5 meter scarp. There is little evidence for compensating uplift in the area. The hanging wall block of the Hebgen fault subsided as much as 6.0 meters. The data suggests an overall fault displacement of 6 meters taken up on two faults. The focal mechanism solution indicated only one fault plane striking at azimuth $280^{\circ} \pm 10^{\circ}$ and dipping $54^{\circ}S \pm 8^{\circ}$ (Ryall, 1962). However, the field data indicates two faults (Fig 2B, 12). In my model the Red Canyon fault dips $54^{\circ}S$ and extends to a depth of 12 km and the Hebgen fault has a dip of $76^{\circ}S$ and extends to the Red Canyon fault, to a depth of about 4 km (Fig 2B).

The best fit earthquake (Fig 14) is obtained by applying slip in the amount revealed by the Red Canyon (4.5 m) and Hebgen (1.5 m) fault scarps to a depth of about 4 km. Between 4-12 km the amount of slip applied is equivalent to the overall subsidence observed, about 6 meters. The model fit is good except for the lack of compensating uplift in the USCGS data. However, the uplift zone is so mountainous that precise elevation changes are difficult to prove (Savage & Hastie, 1966). This model obtained a better fit than dislocation models of Savage and Hastie (1966) because their models used only

Figure 14. Model generated coseismic displacements of selected surface nodal points for the modeled Hebgen Lake earthquake.

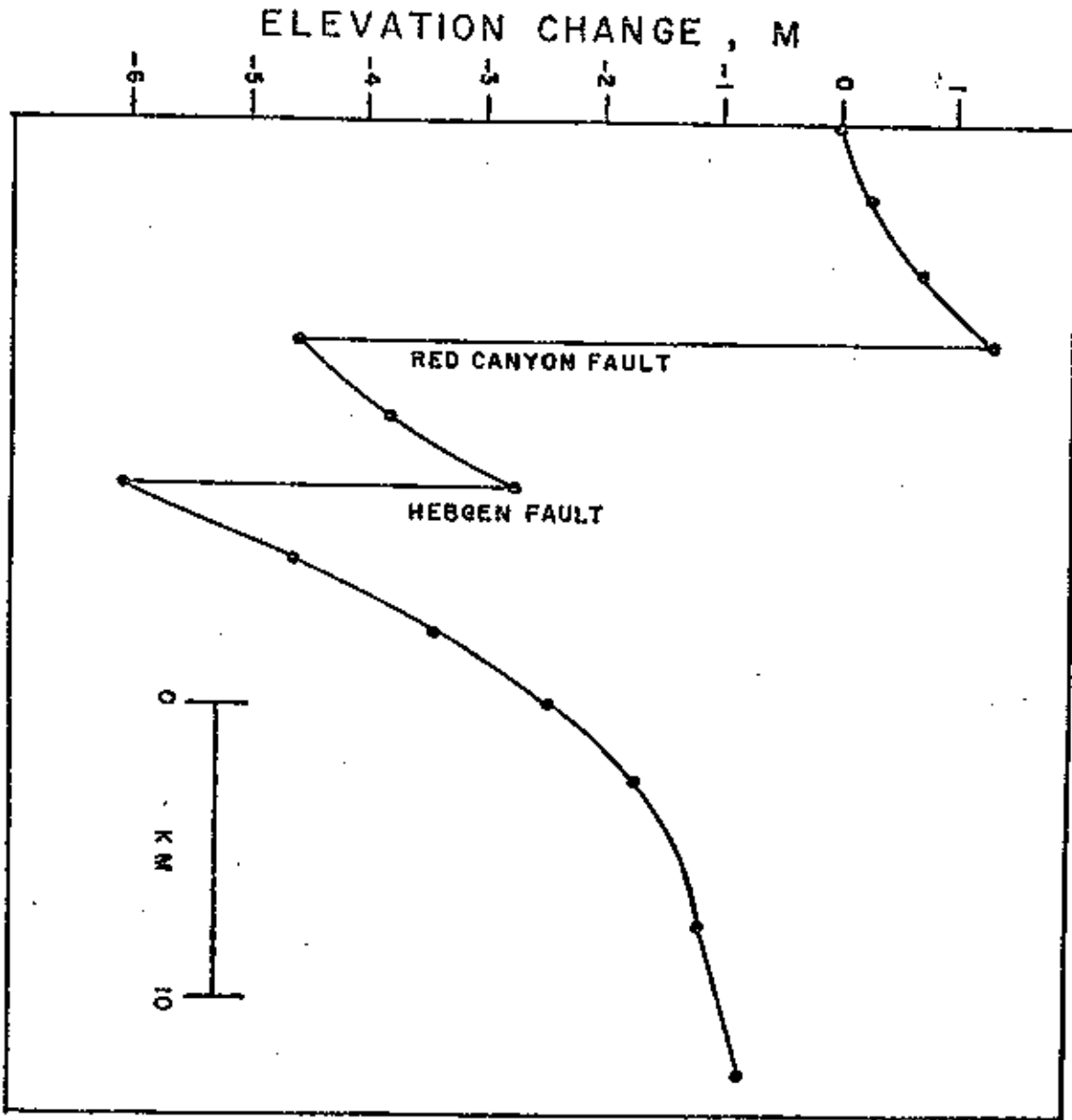


Figure 14

one fault which did not intersect the surface.

The visco-elastic model generated creep strains for the interseismic displacements following the modeled earthquake are shown in Figure 15. The creep strains are caused by a differential tensile stress recovery, as the lithosphere extends above a Maxwell asthenosphere. The rate at which the lithosphere deforms is dependent on the viscosity of the asthenosphere. The viscosity is estimated at 2.3×10^{21} poise based on doming rates of 3-5 mm/yr. This value is close to the viscosity of $1.7-2.4 \times 10^{21}$ poise reported by Cathles (1975) for Lake Bonneville, Utah.

The model generated points suggest that the contemporary or interseismic doming observed in the Hebgen Lake area can result from interseismic strain accumulation (Fig 15). The doming is in the immediate vicinity of the 1959 earthquake. This is not the interpretation of Reilinger et al. (1977). They suggest that the doming is caused by a magma chamber beneath Hebgen Lake-Yellowstone region, however, there is little evidence to support their conclusions. It is likely that voluminous volcanics in the region paralleled normal fault formation; however, it is less probable in view of my results, that magma intrusions into the crust caused the observed doming. Geodetic data for this area is so scarce that any other interpretation based on model results would be inconclusive. Moreover, the

detailed model interseismic fit (Fig 15) is poor compared to the USCGS line BC (Fig 3,13). The most probable reason for the discrepancy is that line BC meanders and is not perpendicular to the 1959 fault scarps.

Figure 15. Model generated interseismic deformation along line AB in figure 12 following the modeled Hebgen Lake earthquake. Doming is centered on the coseismic zone.

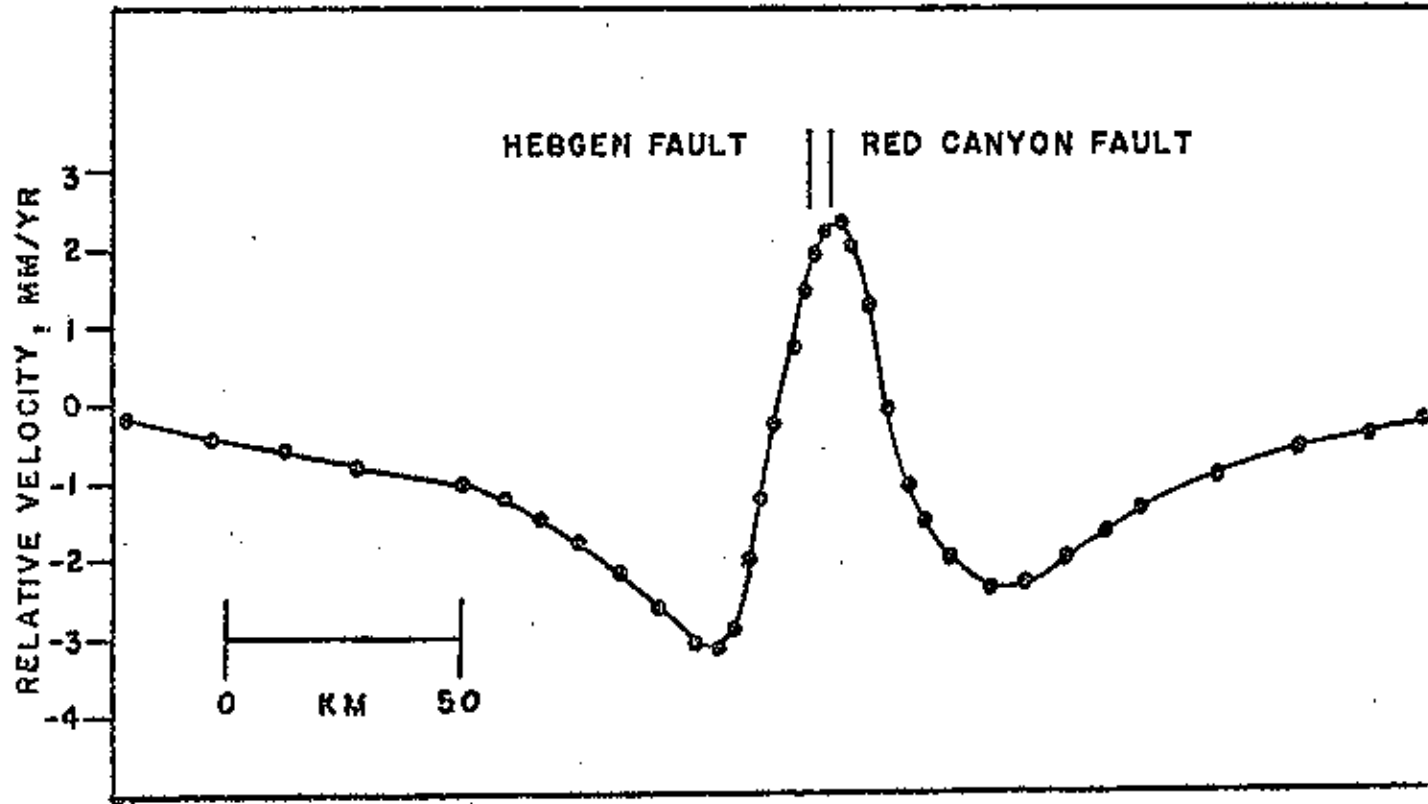


Figure 15

DISCUSSION

A simple model of normal faulting confined to an elastic lithosphere which is being stretched over a viscous asthenosphere can be used to generate normal fault earthquake cycles. The model results are fundamental to the understanding of an earthquake mechanism where crustal deformation is expressed as crustal extension.

The Fairview Peak coseismic and Hebgen Lake coseismic models showed more uplift than was actually observed. The Hebgen Lake model used the interpretation of Savage and Hastie (1966), except this model used two faults, which resulted in a better fit to the surface data. The Fairview Peak exhibited results almost identical to that of Savage and Hastie (1966).

The post-seismic phase from the Fairview Peak data indicates continued slip on faults which occurred between 1955-1967, but the overall trend between 1955-1973 indicates no significant crustal deformation. I suggest that doming is occurring, but due to the high asthenosphere viscosity, the doming is occurring very slowly, on the order of 0.5 mm/yr. The rate of extension of the Basin and Range Province of at least 0.4 mm/yr (Thompson & Burke, 1973) corroborates to model generated extension of 1.36 mm/yr. Interseismic models for Hebgen Lake confirm that the observed doming is consistent with an elastic

rebound model for normal earthquakes.

The only exception to simulated interseismic doming occurs when the simulated faulting extends through the lithosphere. When the dislocation slip extends through the lithosphere the major stress drop occurs in the upper portion of the asthenosphere. Interseismic deformation then results in viscous flow and not an accumulation of stress in the elastic lithosphere in the vicinity of the fault.

However, fault models presented here suggest that faulting is confined to the upper 12 km of the lithosphere. This implies that strain is not accumulating in the lower lithosphere. Artemjev and Artyushkov (1971) postulate that during rifting, stresses will concentrate in the upper portion of the crust. If the tensile strength of this portion of the crust is exceeded a break will occur in the upper crust and the lower portion of a highly viscous lithosphere will spread and produce a neck (Artemjev & Artyushkov, 1971). Similarly, Stewart (1971) has suggested that horsts and grabens in the Basin and Range Province typically fracture only the upper portion of the crust. Furthermore, faults which extend to the lower lithosphere or upper asthenosphere are probably creeping at depth.

The reoccurrence interval for these earthquakes is unknown. There are two obscure reports (Richter, 1958) of an earlier event north of Fairview Peak in 1907 but

the reports are dubious. There are no reports of previous earthquakes at Hebgen Lake. Thus, a statistical reoccurrence interval is impossible.

Thompson and Burke (1971) have examined periodically reactivated fault scarps in Dixie Valley (Fig 4), and suggest an approximate reoccurrence interval based on the rate at which those fault scarps have been effaced by erosion. They suggest the faults in Dixie Valley are reactivated less often than every 100 years but more often than every 10,000 years.

Model generated shear stress recovery can estimate when stresses will return to pre-earthquake levels. The model interseismic stress recovery is on the order of 1000 years for the Fairview Peak and Hebgen Lake faults. A 1000 year reoccurrence interval is compatible with reoccurrence intervals from the intraplate regions of China and Japan (Shimazaki, 1976). The probability of future earthquakes, based on crustal strains, are not possible for these regions because of the scarcity of geodetic data.

It is probable that stresses are recovering very slowly in both areas. Furthermore, it is unlikely that these faults present a current earthquake risk. However, normal faults usually comprise multiple sets of faults in tensile regions. Consequently, other faults in these areas may be approaching earthquake stress levels and

thereby may present potential earthquake hazards.

Geodetic data provides an approximate value for the effective viscosity of the asthenosphere. The rate of interseismic crustal doming is influenced by the viscosity of the asthenosphere. Thus to match model generated interseismic deformation to actual interseismic deformation it was necessary to adjust the viscosity of the asthenosphere. Effective viscosities of $2.1-2.3 \times 10^{21}$ poise obtained in the model are compatible with viscosities determined from Glacial Rebound data, especially from Lake Bonneville, Utah which is in a similar geologic environment (Cathles, 1975). Lake Bonneville lies within the northeastern Basin and Range Province, an active tectonic region. Moreover, the elastic lithosphere thickness must be about 10 km to permit the 65 meters of observed isostatic compensation over the past 4000 years (Crittenden, 1963; Bott, 1971).

SUMMARY

The finite element method (Bischke, 1974) can be used to generate normal fault earthquakes and interseismic secular displacements. The Elastic Rebound model for normal faults is consistent with plate tectonics which demands an elastic lithosphere overlying a viscous asthenosphere.

If the faulting does not extend through the lithosphere, then the interseismic period ground deformation produces relative doming in the vicinity of the fault. Moreover, asthenosphere viscosity influences the rate at which interseismic doming will proceed. The viscosities indicated by the Hebgen Lake and Fairview Peak models of approximately $2.1-2.3 \times 10^{21}$ poise are consistent with Glacial Rebound data for Lake Bonneville, Utah (Cathles, 1975). Doming in normal faulted regions previously has been interpreted by some investigators to represent magma chamber fluctuations. While this may be true in some areas, this work shows that magma chambers need not be invoked to explain the doming.

When the frictional strength of the crust is exceeded, an earthquake will occur accompanied by an abrupt rebound of the crust and a finite stress drop. Model coseismic displacements are consistent with dislocation models of Savage and Hastie (1966).

An approximate recurrence interval for the Hebgen Lake and Fairview Peak faults is found to be on the order

of 1000 years based on interseismic shear stress recovery. This recurrence interval is consistent with the recurrence interval for an intraplate region of Japan (Shimazaki, 1976). Moreover, this recurrence is within the range ($100 < RI < 10,000$) determined by a completely independent method (Thompson & Burke, 1971). Thompson and Burke (1971) suggest that if the recurrence interval was every 1000 years the spreading rate of Dixie Valley would be 1.5 mm/yr. The model generated spreading rate is 1.36 mm/yr. Furthermore, a 1000 year recurrence interval suggests that these intraplate faults are accumulating interseismic stress at a very slow rate, perhaps only a few bars per one hundred years.

BIBLIOGRAPHY

- Armstrong R. L., E. B. Ekren, E. H. McKee, and D. C. Noble, 1969, Space-time relations of Cenozoic silicic volcanism in the Great Basin of the western United States, *Am. J. Sci.*, 267, 478-490.
- Artemjev, M. E., and E. V. Artyushkov, 1971, Structure and isostasy of the Baikal rift and the mechanism of rifting, *J. Geophys. Res.*, 76, 1197-1211.
- Artyushkov, E. V., 1973, Stresses in the lithosphere caused by crustal thickness inhomogeneties, *J. Geophys. Res.*, 78, 7675-7708.
- Bischke, R. E., 1974, A model of convergent plate margins based on the recent tectonics of Shikoku, Japan, *J. Geophys. Res.*, 79, 4845-4857.
- Bischke, R. E., 1976, Secular horizontal displacements: A method for predicting great thrust earthquakes and for assessing earthquake risk, *J. Geophys. Res.*, 81, 2511-2516.
- Bomford, G., 1971, *Geodesy*, 3rd ed., Oxford Clarendon Press.
- Bott, M. H. P., 1971, *The interior of the earth*, St. Martin's Press, New York, 316 p.
- Brown, L. D., and J. E. Oliver, 1976, Vertical crustal movements from leveling data and their relations to geologic structure in the eastern United States, *Rev. Geophys. Space Phys.*, 14, 13-35.

- Brune, J. N., and C. R. Allen, 1967, A low stress drop, low-magnitude earthquake with surface faulting: The Imperial, California earthquake of March 4, 1966, *Bull. Seism. Soc. Am.*, 57, 501-514.
- Byerly, P., 1956, The Fallon-Stillwater earthquakes of July 6, 1954 and August 23, 1954, *Bull. Seism. Soc. Am.*, 46, 1-3.
- Cathles, L. M., III, 1975, The viscosity of the earth's mantle, Princeton University Press, 388 p.
- Crittenden, M. D., Jr., 1963, Effective viscosity of the earth derived from isostatic loading of Pleistocene Lake Bonneville, *J. Geophys. Res.*, 68, 5517-5530.
- Eaton, J. P., 1963, Crustal structure from San Francisco, California, to Eureka, Nevada, from seismic-refraction measurements, *J. Geophys. Res.*, 66, 5789-5806.
- Elsasser, W. M., 1969, Convection and stress propagation in the upper mantle, in *The Application of Modern Physics to the Earth and Planetary Interiors*, edited by W. K. Runcorn, pp. 223-264, Interscience, New York.
- Fitch, T. J., and C. H. Scholz, 1971, Mechanism of underthrusting in southwest Japan: A model of convergent plate interactions, *J. Geophys. Res.*, 76, 7260-7292.
- Fraser, G. D., I. J. Witkind, and W. H. Nelson, 1964, A geological interpretation of the epicentral area—The dual basin concept, *U. S. Geol. Surv. Prof.*

- Pap., 435, pp. 99-106.
- Green, D. H., and A. E. Ringwood, 1972, A comparison of recent experimental data on the gabbro-garnet granulite-eclogite transition, *J. Geol.*, 80, 277-288.
- Gumper, F. J., and C. Scholz, 1971, Micro-seismicity and tectonics of the Nevada seismic zone, *Bull. Seism. Soc. Am.*, 61, 1413-1432.
- Hamilton, W., and W. B. Myers, 1966, Cenozoic tectonics of the western United States, *Rev. Geophys. Space Phys.*, 4, 509-549.
- Hobbs, B. E., W. D. Means, and P. F. Williams, 1976, An outline of structural geology, Wiley, New York, 571 p.
- Holdahl, S. R., 1973a, Vertical crustal movements-Status of NGS investigations, paper presented at Geop-3 Research Conference: Vertical crustal movements and their causes, AGU, Washington, D. C.
- Jacoby, W. R., 1970, Instability in the upper mantle and global plate movements, *J. Geophys. Res.*, 75, 5671-5680.
- Kanamori, H., and D. L. Anderson, 1975, Theoretical basis of some empirical relations in seismology, *Bull. Seism. Soc. Am.*, 65, 1073-1095.
- Karig, D. E., 1971a, Origin and development of marginal basins in the western Pacific, *J. Geophys. Res.*, 76, 2542-2561.

- Maruyama, T., 1964, Statical elastic dislocations in an infinite and semi-infinite medium, Bull. Eqk. Res. Inst., Tokyo Univ., 42, 289-368.
- McKenzie, D. P., and F. Richter, 1976, Convection currents in the earth's mantle, Sci. Amer., 78, 72-90.
- Meister, L. J., R. O. Burford, G. A. Thompson, and R. L. Kovach, 1968, Surface strain changes and strain energy release in the Dixie Valley - Fairview Peak area Nevada, J. Geophys. Res., 73, 5981-5994.
- Molnar, P., and J. Oliver, 1969, Lateral variations of attenuation in the upper mantle and discontinuities in the lithosphere, J. Geophys. Res., 74, 2648-2682.
- Morgan, W. J., 1972, Deep mantle convection plumes and plate motions, Amer. Assn. Petrol. Geol. Bull., 56, 203-213.
- Myers, W. F., and W. Hamilton, 1964, Deformation accompanying the Hebgen Lake earthquake of August 17, 1959, U. S. Geol. Surv. Prof. Pap., 435, 55-98.
- Pakiser, L. C., and I. Zietz, 1965, Transcontinental crustal - mantle structure, Rev. Geophys. Space Phys., 3, 505-520.
- Plafker, G., 1972, Alaskan earthquake of 1964 and Chilean earthquake of 1960: Implications for arc tectonics, J. Geophys. Res., 77, 901-925.

- Prodehl, C., 1970, Seismic refraction study of crustal structure in the western United States, Bull. Seism. Soc. Am., 81, 2629-2646.
- Reid, H. F., 1910, The mechanics of the earthquake, in The California Earthquake of April 18, 1906, Report of the State Earthquake Investigation Commission, 2, pp. 16-28, Carnegie Institution, Washington, D. C.
- Reil, O. E., 1957, Damage to Nevada highways, Bull. Seism. Soc. Am., 47, 349-352.
- Reilinger, R. E., G. P. Citron, and L. D. Brown, 1977, Recent vertical crustal movements from precise leveling data in southwestern Montana, western Yellowstone National Park, and the Snake River Plain, J. Geophys. Res., 82, 5349-5359.
- Richter, C. F., 1958, Elementary Seismology, Freeman, San Francisco, 768 p.
- Romney, C., 1957, Seismic waves from the Dixie Valley Fairview Peak earthquakes, Bull. Seism. Soc. Am., 47, 301-319.
- Roy, R. F., E. R. Decker, D. D. Blackwell, and F. Birch, 1968, Heat flow in the United States, J. Geophys. Res., 73, 5207-5221.
- Savage, J. C., and L. M. Hastie, 1966, Surface deformation associated with dip slip faulting, J. Geophys. Res., 71, 4897-4904.
- Savage, J. C., and L. M. Hastie, 1969, A dislocation

- model for the Fairview Peak, Nevada, earthquake,
Bull. Seism. Soc. Am., 59, 1937-1948.
- Savage, J. C., and J. P. Church, 1974, Evidence for
postearthquake slip in the Fairview Peak, Dixie
Valley, and Rainbow Mountain fault areas of Nevada,
Bull. Seism. Soc. Am., 64, 687-698.
- Sbar, M. L., M. Barazangi, J. Dorman, C. H. Scholz,
and R. B. Smith, 1972, Tectonics of the inter-
mountain seismic belt, western United States
microearthquake seismicity and composite fault
plane solutions, Geol. Soc. Am. Bull., 83, 13-28.
- Sbar, M. L., and L. R. Sykes, 1973, Contemporary
compressive stress and seismicity in eastern
North America: An example of Intra-plate tectonics,
Geol. Soc. Am. Bull., 84, 1861-1882.
- Scholz, C. H., 1972, Crustal movements in tectonic
areas, Forerunners of strong earthquakes, Tectono-
physics, 14, 201-217.
- Scholz, C. H., M. Barazangi, and M. L. Sbar, 1971,
Late Cenozoic evolution of the Great Basin, western
United States, as an ensialic interarc basin,
Geol. Soc. Am. Bull., 82, 2979-2990.
- Scholz, C. H., and T. J. Fitch, 1969, Strain accumulation
along the San Andreas fault, J. Geophys. Res.,
74, 6649-6666.
- Scholz, C. H., and T. J. Fitch, 1970, Strain and creep

- in central California, *J. Geophys. Res.*, 75,
4447-4453.
- Scholz, C. H., and T. Kato, 1978, The behaviour of a
convergent plate boundary, *J. Geophys. Res.*, 83,
783-797.
- Seegerlind, L. J., 1976, *Applied finite element analysis*,
Wiley, New York, 412 p.
- Slemmons, D. B., 1957, Geological effects of the Dixie
Valley - Fairview Peak, Nevada, earthquakes of
December 16, 1954, *Bull. Seism. Soc. Am.*, 47,
353-375.
- Shimazaki, K., 1976, Intraplate seismicity gap along
the Median Tectonic Line and oblique plate
convergence in southwestern Japan, *Tectonophysics*,
31, 139-156.
- Smith, P. J., 1973, *Topics in geophysics*, MIT Press,
Mass., 246 p.
- Smith, R. B., and M. L. Sbar, 1974, Contemporary
tectonics and seismicity of the western United
States with emphasis on the intermountain seismic
belt, *Geol. Soc. Am. Bull.*, 85, 1205-1218.
- Stewart, J. H., 1971, Basin and Range structure: A
system of horsts and grabens produced by deep-
seated extension, *Geol. Soc. Am. Bull.*, 82, 1019-
1044.
- Thompson, G. A., 1959 *Gravity measurements between*

- Hazen and Austin, Nevada: A study of Basin-Range structure, *J. Geophys. Res.*, 64, 217-229.
- Thompson, G. A., and D. B. Burke, 1973, Rate and direction of spreading in Dixie Valley, Basin and Range Province, Nevada, *Geol. Soc. Am. Bull.*, 84, 627-632.
- Trimble, A. B., and R. B. Smith, 1975, Seismicity and contemporary tectonics of the Hebgen Lake - Yellowstone region, *J. Geophys. Res.*, 80, 733-741.
- Whitten, C. A., 1957, Geodetic measurements in the Dixie Valley area, *Bull. Seism. Soc. Am.*, 47, 321-325.
- Zienkiewicz, O. C., M. Watson, and I. P. King, 1968, A numerical method of viscoelastic stress analysis, *Int. J. Mech. Sci.*, 10, 807-827.